Continuous theta-burst stimulation of the prefrontal cortex in the macaque monkey: no evidence for within-target inhibition or cross-hemisphere disinhibition of neural activity

Running head: cTBS in macaque monkey prefrontal cortex

Sebastian J Lehmann[1] and Brian D Corneil[1-3],

[1]Department of Physiology & Pharmacology, Western University, London, ON, Canada, N6A 5B7
[2]Department of Psychology, Western University, London, ON, Canada, N6A 5B7
[3]Robarts Research Institute, Western University, London, ON, Canada, N6A 5B7

Corresponding Author: Brian D Corneil, bcorneil@uwo.ca

Number of pages: 44
Number of figures: 9
Number of tables: 1
Number of words: Abstract: 236 Introduction: 1025 Discussion: 2812

Keywords: TMS, continuous theta burst stimulation, pre-frontal cortex, macaque

Acknowledgements: This work was supported by Operating Grants from the Canadian Institutes of Health Research (CIHR; MOP-123247, MOP-142317, PJT-186160). We thank Dr. Julio Martinez-Trujillo for surgical expertise during the insertion of the Utah arrays.

Abstract

Continuous theta-burst stimulation (cTBS) can perturb neural activity and behavior by inducing effects that persist beyond the relatively short stimulation period. Although widely used in basic research and clinical settings, there lacks an understanding of the neurophysiological and behavioural effects of cTBS. Two assumptions motivating the use of cTBS are that it will i) inhibit neural activity in the targeted area, and ii) consequently disinhibit neural activity in the mirroring region in the contralateral cortex. Here, we test these assumptions in the oculomotor system of the rhesus macaque. In two macaques, we delivered cTBS between blocks of trials where they performed a delayed pro-/anti-saccade task, delivered cTBS to the right PFC (areas 8Ar and 46, which includes the frontal eye fields; 32 *cTBS-PFC* sessions), to the air as a SHAM control (27 *cTBS-SHAM* sessions), or to the nearby primary motor cortex as a brain control (21 *cTBS-M1* sessions). Across these different types of sessions, we compared changes in oculomotor behavior (reaction times, error rates, peak saccade velocity), and changes in neural activity recorded from the left, contralateral PFC. Despite multiple lines of evidence consistent with TMS influencing neural activity in the cTBS-PFC and cTBS-M1 sessions, we found no behavioral evidence for inhibition of the right PFC in the cTBS-PFC sessions, nor any evidence for contralateral disinhibition in the left PFC. Our results call into question some of the fundamental assumptions underlying the application of cTBS.

Introduction

Transcranial magnetic stimulation (TMS) is one of the most common forms of non-invasive brain stimulation. TMS is widely used in both basic research and clinical scenarios, offering a reliable means to manipulate cortical activity in a targeted and non-invasive manner. Repetitive forms of TMS such as theta burst stimulation (TBS) are particularly intriguing, as they induce neural effects that persist for some time after its application. For example, continuous theta-burst stimulation (cTBS) is thought to transiently decrease neural activity in the targeted area. Such effects were first reported

in primary motor cortex (M1, Huang et al., 2005, 2017), but cTBS is now routinely applied to any number of brain areas (Franca *et al.*, 2006; Rahnev *et al.*, 2013; Hanlon *et al.*, 2015; Valchev *et al.*, 2015; Blumberger *et al.*, 2018; Strzalkowski *et al.*, 2019). Doing so assumes that the effects of cTBS-M1 will generalize to other brain areas, and that such effects will modulate activity within anatomically and functionally connected regions. Indeed, one common assumption motivating its use is that cTBS-induced inhibition of the targeted brain area will increase, via disinhibition, activity in the mirroring, callosal targets (Mochizuki *et al.*, 2007; Stefan *et al.*, 2008; Suppa *et al.*, 2008, 2016; Lefaucheur *et al.*, 2020). The idea that repetitive TMS can 'rebalance' activity across hemispheres via ipsilateral inhibition and contralateral disinhibition have motivated its exploration as a treatment mode following stroke (Zheng, Liao and Xia, 2015; Li *et al.*, 2016; Long *et al.*, 2018; Vink *et al.*, 2023) or intractable depression (George *et al.*, 2010; Li *et al.*, 2014; Kang *et al.*, 2016; Brunoni *et al.*, 2017; Theleritis *et al.*, 2017).

Despite widespread use there remains a gap in knowledge in the precise neurophysiological effects of cTBS both in the targeted area and in interconnected areas, and a series of recent results in humans have questioned the reliability of effects of repetitive TMS protocols (Hamada *et al.*, 2013; Hordacre *et al.*, 2017; Perellón-Alfonso *et al.*, 2018; Boucher *et al.*, 2021; Magnuson *et al.*, 2023). Recent consensus statements (Edwards *et al.*, 2024) emphasize the importance of animal models in helping bridge the gap in knowledge. We and others (Gerits *et al.*, 2011; Mueller *et al.*, 2014; Balan *et al.*, 2017; Romero *et al.*, 2019, 2022; Pouget *et al.*, 2020; Klink *et al.*, 2021; Lehmann and Corneil, 2022; De Lima-Pardini *et al.*, 2023) have argued that the non-human primate (NHP) macaque offers an excellent animal model, given homologies in cortical microstructure, gyrification, and the anatomy and function of distributed brain networks to those found in humans. The oculomotor system can offer a particularly useful network to study in this animal model, given similarities in retinal structure and oculomotor repertoire to humans, and the extensive work in the rhesus macaque that has detailed patterns of neural activity associated with the performance of complex behavioral tasks (Lehmann and Corneil, 2022). Further, the

macaque oculomotor system has been studied with many causal techniques, such as microstimulation (Robinson and Fuchs, 1969; Robinson, 1972; Bruce *et al.*, 1985), cryogenic (Peel *et al.*, 2017, 2020; Dash *et al.*, 2018; Johnston, Lomber and Everling, no date) or pharmacological inactivation (Sommer and Tehovnik, 1997; Dias and Segraves, 1999), or permanent lesions (Schiller, Sandell and Maunsell, 1987; Kunimatsu *et al.*, 2015; Adam *et al.*, 2020), providing a grounding for how non-invasive brain stimulation techniques like cTBS should influence brain and behavior.

The focus of this current study is on the prefrontal cortex (PFC), and specifically the areas rostral to and including the anterior bank of the arcuate sulcus that includes the frontal eye fields (FEF) and adjacent area 8Ar/46. This area has been extensively targeted with TMS in humans (for a review, see Vernet et al., 2014) and in macaques (Gerits *et al.*, 2011; Valero-Cabre *et al.*, 2012; Gu and Corneil, 2014; Mueller *et al.*, 2014; Balan *et al.*, 2017). These frontal areas are reciprocally connected anatomically with their callosal target (Schwartz and Goldman‐Rakic, 1984), and neurophysiological results in NHPs support the notion of crossed-hemisphere inhibition (Schlag, Dassonville and Schlag-Rey, 1998; Cohen *et al.*, 2010; Ramezanpour *et al.*, 2024). The PFC of the rhesus macaque therefore offers an excellent platform to test the two assumptions that cTBS-PFC will i) inhibit neural activity in the targeted area, and ii) consequently disinhibit neural activity in the mirroring, contralateral PFC (Fig. 1A).

To test these predictions, we investigated the behavioral and neurophysiological effects of cTBS-PFC in two rhesus macaques performing a memory-guided saccade task that required them to remember the rule to generate a pro- (look toward) or anti- (look away from) a flashed target upon disappearance of a central fixation point. This task requires working memory for a rule that needs to be applied in the future, as well as stimulus encoding and motor execution, all of which influence the activity of PFC neurons (Bullock *et al.*, 2017; Backen, Treue and Martinez-Trujillo, 2018). We used a block design, comparing behavior and neural activity before and after cTBS-PFC to that observed with intervening bouts of cTBS delivered either to the air (termed cTBS-SHAM, to control for acoustic effects) or cTBS delivered to the nearby hand area

of motor cortex (termed cTBS-M1, serving as a brain control that does not target the oculomotor network but controls for tactile sensations arising from TMS). The hypothesis that cTBS i) inhibits neural activity in the targeted PFC predicts increases in error rates and saccade latency and decreases in saccade velocity, as such effects are commonly observed with inactivation or lesion of the frontal cortex (Bruce *et al.*, 1985; Sommer and Tehovnik, 1997; Dias and Segraves, 1999; Peel *et al.*, 2014), particularly during the execution of more cognitively-demanding tasks (Pierrot-Deseilligny *et al.*, 1991; Pierrot-Deseilligny *et al.*, 2003; Peel *et al.*, 2017). The hypothesis that cTBS-mediated inhibition will ii) disinhibit the contralateral target predicts increased neural activity in the mirroring target, hence we also recorded from the PFC contralateral to the side of cTBS via a chronically-implanted array.

Across an extensive database collected from two animals, we found no behavioral or neural effects that could be reliably attributed to a perturbation of PFC and/or a change of spiking activity in the mirroring, contralateral target.

Methods

Subjects and surgical procedures

The experiments were performed in two male adult rhesus macaques (*Macaca mulatta*, animals Bu and Gr, 7 and 9 years old, weighing ca. 11 and 9 kg, respectively). Animal housing, training, surgical, and experimental procedures were approved by the Animal Use Subcommittee of the University of Western Ontario Council on Animal Care, and were conducted in accordance with the Canadian Council on Animal Care policy on the use of laboratory animals, which conforms to the guidelines laid down by the National Institutes of Health regarding the care and use of animals for experimental procedures. The NHPs' health and weight were monitored daily. Each macaque underwent two surgeries. In the first surgery, a head post was implanted to restrain head motion during training and recordings sessions, along with several fiduciary markers for neuro-navigation embedded in the acrylic implant. The implant was secured to the skull using titanium and ceramic screws, with the ceramic screws placed in the anterior part

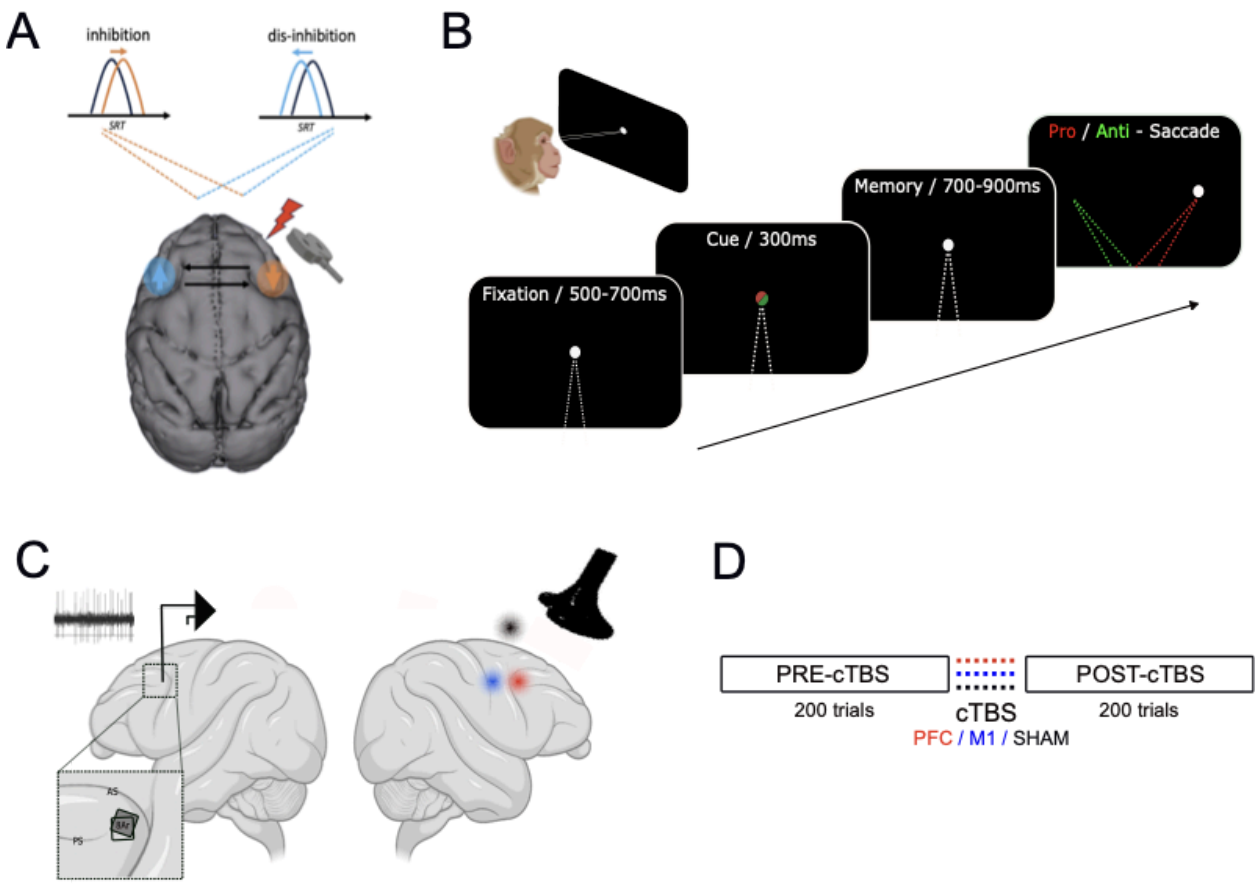

Figure 1. Methods A. cTBS is expected to inhibit neural activity in the targeted right PFC and disinhibit activity in the contralateral left PFC, potentially impacting behavioral markers such as error rate, saccadic reaction time and peak velocity, and spiking activity in the contralateral PFC. **B.** Two rhesus macaques performed a delayed pro- and anti-saccade task with a working memory component, requiring saccades toward or away from a target appearing on the left or right, resulting in four conditions. **C.** cTBS was delivered in separate daily sessions to either the right PFC (red), right M1 (blue), or as a SHAM control (black, 2 cm above the right hemisphere). Neural activity was recorded from multielectrode arrays in the left PFC-8Ar area, rostral to the arcuate sulcus and caudal to the principal sulcus. Individual positions for monkeys Bu (opaque) and Gr (grey) are shown in the magnified section. **D.** In a blocked design, the monkeys first completed 200 trials (50 per condition) of the task (PRE-cTBS), followed by cTBS delivery, and then immediately completed a second set of 200 trials (POST-cTBS).

of the skull where TMS would be delivered. The thickness of the acrylic above the areas of interest for delivery of TMS was limited to ~5 mm to ensure a minimal distance to the cortical surface (for more details see Gu and Corneil, 2014). Animals then underwent structural MRI scans to confirm cortical landmarks and locate the embedded fiduciary markers, serving for surgical planning and the use of neuro-navigation techniques for precise positioning of the TMS coil (described in detail below). In a second surgery, a multi-electrode Utah array (Blackrock Microsystems, 96 channels, electrode length

1.5mm, 10-by-10 design with 400 micrometer inter-electrode spacing) was implanted in the left (contralateral to the side of cTBS) prefrontal cortex, caudal to the posterior end of the principal sulcus and anterior to the principal sulcus (see Fig. 1C for array locations in both animals, for additional technical details see Bullock *et al.*, 2017). Recordings were started after a recovery period of 2 to 3 weeks.

Behavioural Task. In the time between the two surgeries, the macaques were trained to comfortably sit upright in an individually adjusted primate chair, with their head restrained, facing a board of LEDs while sitting in a dark, secluded experimental room. They were trained to perform a delayed pro- and anti-saccade task, which required them to hold in working memory the rule to look either toward (*pro-saccade*) or away from (*anti-saccade*) an upcoming peripheral stimulus (Fig.1B), and then apply this rule when the peripheral stimulus was presented. The task was controlled via custom written real-time LabView programs (NI-PXI controller, National Instruments, 1kHz sampling rate), and the position of the left eye was measured by a remote eye tracking system (ETL-200, 120 Hz sampling rate, ISCAN Inc, USA). Each trial began with the presentation of a central orange LED, which the animal had to fixate for a variable period of 500-700 ms, with a tolerance of ~3 deg radius. The color of this central LED then changed briefly for 300 ms to either red or green, which cued the monkey to plan for an upcoming pro-saccade (red instructional cue) or anti-saccade (green instructional cue). The monkey had to maintain central fixation during this time. The central LED then changed back to orange for a period of 700-900 ms, and during this time the animal had to remember the rule for the current trials while maintaining fixation on the central target. The central LED was then turned off and at the same time a peripheral red target was turned on either 15 degrees of visual angle to the left or right. The monkey was rewarded with a small amount of fluid if they executed the correct pro- or anti-saccade within 500 ms of target appearance, and remained for 200ms within the target window ~(5 deg radius). With this experimental structure, there are four unique trial types (pro- vs anti-, stimulus presentation left or right), which were presented pseudo-randomly interleaved. On average, the monkeys conducted approximately 9 and 11 trials per

minute (monkeys Bu and Gr, respectively). The amount of reward was kept constant within a given experimental session.

As illustrated in Fig 1D, data on any given day were collected within an experimental session that consisted of ~200 correctly executed trials before cTBS (~50 of each unique trial type, termed 'PRE-cTBS'), followed by delivery of cTBS, followed immediately by another ~200 correctly executed trials (~50 of each unique trial type, termed 'POST-cTBS'). cTBS always consisted of 600 pulses of TMS, delivered in bursts of 3 pulses at 50 Hz, with an inter-burst frequency of 5 Hz (40 seconds in total). cTBS was delivered to one of three targets on any given recording day, these being: the prefrontal cortex (cTBS-PFC), the hand area of motor cortex (cTBS-M1, serving as a brain control, and a control for tactile sensations and acoustic effects), or 2 cm above the head (cTBS-SHAM, which controls for acoustic effects). Depending on the animals' individual performance rates, the complete PRE-cTBS and POST-cTBS intervals each lasted for between 20 to 25 minutes. In both monkeys, we initially alternated sessions of cTBS-PFC and -SHAM, introducing cTBS-M1 sessions as a second control only after collecting a sufficient number of the initial conditions (after approximately 17 weeks in monkey Bu, and 5 weeks in monkey Gr).

Neuronavigation and Transcranial Magnetic Stimulation. To ensure consistent positioning of the TMS coil above the targeted brain areas, we used a neuronavigation system (cortEXplore, Austria) along with structural MRI scans. For each session, the fiduciary markers embedded within the acrylic implants were used to register the monkey's head to a 3D model obtained from the MRI scans. This allowed us to precisely track and position the TMS coil relative to the cortical target areas in real-time. Biphasic pulses of TMS were applied via a MagStim Rapid Transcranial Magnetic Stimulator with a figure-eight coil originally designed for peripheral nerve stimulation (25 mm inner coil radius; MagStim, UK) and previously used for a variety of NHP studies (Amaya *et al.*, 2010; Gerits *et al.*, 2011; Valero-Cabre *et al.*, 2012; Gu and Corneil, 2014; Romero *et al.*, 2019, 2022). At the beginning of each session, the coil was first positioned above the hand area of the right primary motor cortex (M1) to confirm the

accuracy of neuronavigation, and to confirm the repeatability of the effects of single-pulse TMS across days. Before the start of data collection, 5-10 single pulses of TMS were delivered to M1 at an output setting of 30% (monkey Bu) or 32% (monkey Gr), which reliably evoked visible thumb twitches in the contralateral (left) hand on between 80-100% of attempts (see supplementary video S1 for demonstration). After this, the TMS coil was either kept in place for cTBS-M1 sessions, or adjusted for targeting PFC (~8mm rostral to M1, again using neuronavigation), where single pulses at the same intensity were confirmed to evoke either none or less than 20% hand twitches. We estimate that the output setting used for cTBS was ~110% relative to resting motor threshold, and the observation of qualitatively different evoked responses from the -PFC vs -M1 locations confirms a degree of focality that is consistent with previous reports (Gu and Corneil, 2014). For cTBS-SHAM control sessions, the coil was positioned above the acrylic implant, placing it on a 2cm plastic spacer which was in secure contact with the acrylic implant; in this way, TMS pulses in cTBS-SHAM sessions also delivered a mechanical sensation. In all cases, the coil was locked in place by a clamp anchored to the head post. During cTBS-delivery, the TMS coil was cooled with a combination of air suction and iced water in order to prevent overheating. To avoid potential long-term accumulation of physiological effects, we did not run repeated cTBS-PFC or -M1 sessions on back-to-back days, but instead always followed a day with cTBS-PFC with either one of the control sessions (e.g., either cTBS-SHAM or cTBS-M1), or a day where data was not recorded. Thus, there was a minimum of 48 hours between repeated cTBS-PFC or cTBS-M1 sessions.

Data acquisition and analysis. Neural activity was recorded using a 128-channel Omniplex D neural data acquisition system (Plexon Inc). Neural signals were acquired and digitized at the headstage (16 bit resolution, Plexon DigiAmp), sampled at 40 kHz per channel, with bandpass filtering applied online (300–8000 Hz). All data were stored for offline spike sorting using principal component analysis techniques (Offline Sorter, Plexon Inc) ,the resulting spike time information was then imported into Matlab and aligned to behavioral events. Analog data (including horizontal and vertical eye movement traces and stimulus presentation) was recorded at 1kHz resolution. Data was

analyzed offline using custom-written scripts in MATLAB (MathWorks). Saccade onset (saccadic reaction time, relative to target stimulus onset) and offset were detected by applying a velocity criterion (>50 degree per second), trials with eye blinks or unstable fixation were removed from the database. Peak saccadic velocity was defined as the maximum velocity between saccade on and offset.

Spiking activity. The spiking activity of each recorded neuron was aligned to three task events on a trial-by-trial basis: rule cue onset, target onset, and saccade onset. Peristimulus time histograms (PSTHs) were computed using a causal smoothing kernel based on a gamma distribution (Baumann et al. 2009). Neurons were included for subsequent analyses if they exhibited an average firing rate of at least 1 Hz across all correct trials in at least one of those alignments. To account for variability in overall firing rates across neurons, each unit's firing rate was normalized by dividing by the maximum average firing rate observed in any of the four task conditions (L-pro, R-pro, L-anti, R-anti). Task modulation and selectivity for each epoch were assessed using one-way ANOVAs ($p < 0.01$), comparing spike rates within specific analysis windows for the following condition pairs: (1) pro- vs. anti-saccades during the rule epoch (200–300 ms after cue onset), (2) left vs. right target locations during the visual response epoch (75–150 ms after target onset), and (3) leftward vs. rightward saccades during the peri-saccadic epoch (−50 to +50 ms around saccade onset).

Statistical analyses. Behavioral data analysis of saccade parameters was conducted in Matlab (MathWorks Inc.), while statistical analyses were performed using linear mixed models in Jamovi (v 2.3.28). Separate models were run for behavioral and neural data from each monkey to quantify main and interaction effects; the Satterthwaite method was used to estimate degrees of freedom and p-values. For significant interactions, post-hoc comparisons were made using Bonferroni-adjusted p-values to correct for multiple comparisons. The models assessed the effects of cTBS location (cTBS-PFC, -SHAM, -M1), trial type (pro- vs. anti-), and saccade direction (left vs. right, for the visual response and saccade epochs), with sessions (for behavioral analyses) and unit IDs (for spike rate analyses) included as random effects.

Data visualization. Final figures were generated using standard matlab plotting functions and the “gramm data visualization toolbox” (Morel, 2018). Parts of the Methods figure (Fig. 1) was created using “biorender.com”.

Results

Two rhesus macaques performed an eye movement task in which the instruction to execute a pro- or anti-saccade had to be memorized until the appearance of the visual target, which served as a “go” signal for saccade execution (see *Methods* for details). After ~200 correct trials (i.e., ~50 per condition), 600 pulses of cTBS were delivered to either PFC, M1 (serving as “brain-control”), or above the head (SHAM-control), followed by a second block of the same number of trials. Sessions were limited to one per day, recorded across a total of 23 (monkey Gr) and 13 weeks (monkey Bu), totalling 80 sessions where cTBS was delivered either to the right PFC (17 and 15 sessions for monkey Gr or Bu, respectively), right M1 (11/10), or to the air (a SHAM control, 16/11).

In the following, we first examine saccade error rate, reaction time, and peak velocity to assess whether there are signatures of inhibition following cTBS to the right PFC. For each of these behavioural metrics, we reasoned that bilateral saccade performance could be influenced if cTBS disrupted the encoding or maintenance of the rule to execute a pro- or anti-saccade. Alternatively, unilateral saccade performance could be influenced if cTBS disrupted the processing of leftward visual stimuli (L-pro or R-anti), or the generation of leftward, i.e., contralateral, saccades (L-pro or L-anti). Our hypothesis predicted that such effects would be specific for cTBS-PFC but not cTBS-M1 or cTBS-SHAM, and greater on anti- vs pro-saccade trials. For these behavioural analyses, we compare the pre-post changes observed with cTBS-PFC to those observed for cTBS-M1 and cTBS-SHAM.

Following our behavioural analyses, we then present an analysis of spiking activity recorded from the left PFC, segregating our analysis of neural activity in segments associated with rule maintenance, target onset, and saccade execution.

Behavioral analyses

Error rates. We derived error rates for pro- and anti-saccades in each direction, doing so separately for the pre- and post-cTBS intervals for each of the three areas targeted by cTBS (Fig. 2A&B; red and green colors depict data for pro- and anti-saccades before cTBS respectively, with darker shades for saccades to the right; grey bars show the post-cTBS intervals). As expected from the additional complexity of remembering and executing an anti-saccade, error rates in both monkeys before cTBS were ~5-15% higher on anti- vs pro-saccade trials. The change in error rate across cTBS can be appreciated by comparing these colored bars to the grey bars immediately to the right.

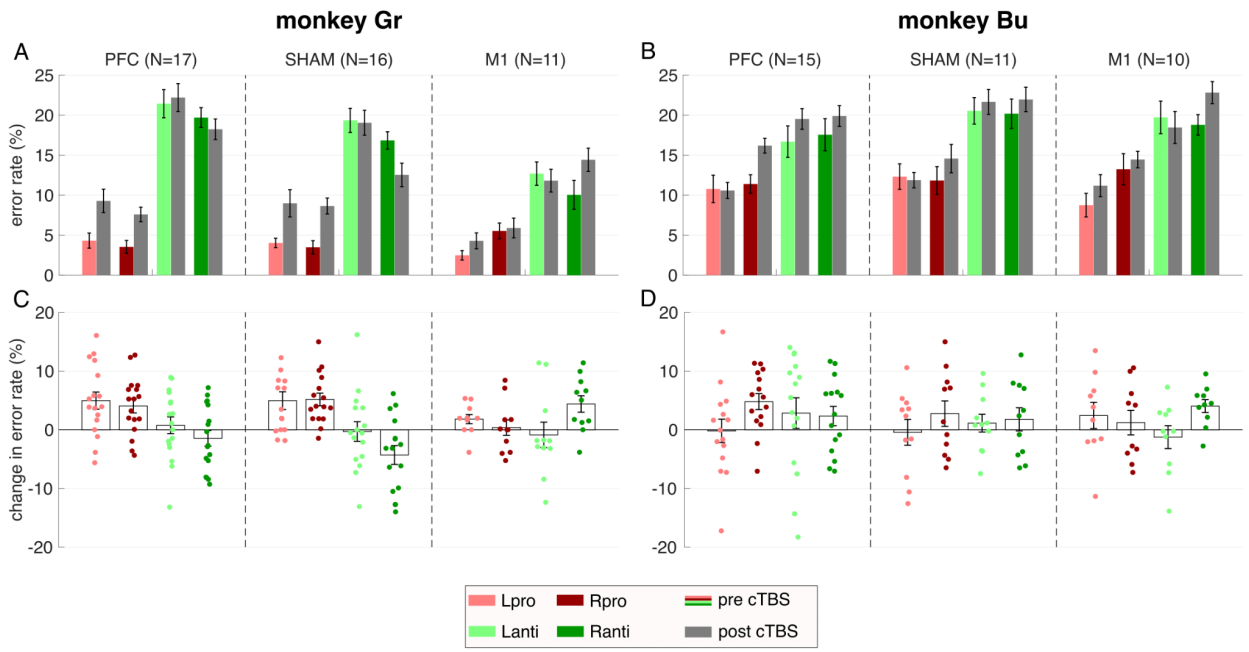

Fig.2 Effect of cTBS on error rates. In these and ensuing plots, the colours indicate task type (red: pro-saccades, green: anti-saccades), while lightness indicates saccade direction (light: leftwards, dark: rightwards). **A,B**. Error rates before (i.e., baseline, coloured bars) and after (grey) cTBS for both monkeys, averaged across sessions (error bars: SEM). **C,D**. Changes in error rate after cTBS delivery (positive values denote an increase in error rate after cTBS). Individual dots indicate the error rate change in a given session, while grey bars represent average change across sessions (error bars: SEM).

Our specific interest is how performance changes across cTBS, as a function of cTBS delivery location, saccade type, and saccade direction. For every session, we therefore derived the change in error rate across cTBS (Fig. 2C&D). To analyze these data, we used a linear mixed model to investigate the effect of cTBS location (cTBS-PFC,

-SHAM, -M1), trial type (pro or anti), and saccade direction (left or right), with individual "sessions" as a random factor. Importantly, we observed no clear evidence that the change in error rate varied as a function of where cTBS was applied, as there was no main effect for cTBS location in either monkey (monkey Gr: $F(2) = 0.19$, $p=0.83$, means PFC = 2.08% ± 0.88, SHAM = 1.38% ± 0.91, M1 = 1.42% ± 1.09; monkey Bu: $p=0.72$, means PFC = 2.45% ± 0.95, SHAM = 1.30% ± 1.11, M1 = 1.61% ± 1.17). In monkey Bu, there were no significant main or interaction effects for any of the tested factors on error rate difference, including cTBS location ($F(2)=0.34$, $p=0.72$) , Fig 2D). In contrast, monkey Gr showed a significant main effect of saccade type ($\beta = -1.93$, SE = ± 0.38, $p_{adj} < 0.001$, 95% CI [-2.67 -1.19]), with larger error rate changes for pro-saccades (3.55% ± 0.67) than anti-saccades (–0.3% ± 0.67; Fig. 2C). There was also a significant interaction between cTBS location and saccade type ($\beta = 4.01$, SE = 0.96, $p < .001$, 95% CI [2.13, 5.09]). Post-hoc tests showed this effect was driven by differences following cTBS to PFC ($p_{adj} = 0.001$; pro = 4.51% ± 1.06, anti = –0.35% ± 1.06) and SHAM ($p_{adj} < .001$; pro = 5.06% ± 1.09, anti = –2.30% ± 1.09), but not M1 ($p = 1.00$; pro = 1.09% ± 1.32, anti = 1.76% ± 1.32). We attribute this to potential overtraining, as M1 sessions were introduced later, coinciding with reduced pro-saccade errors. Additionally, a three-way interaction between cTBS location, saccade type, and saccade direction was significant ($\beta = 2.73$, SE = 0.96, $p = .005$, 95% CI [0.84, 4.62]), driven by larger error rate changes for rightward pro-saccades (5.16% ± 1.40) versus rightward anti-saccades (–4.30% ± 1.40) in the SHAM condition. In summary, there was no evidence for changes in error rate that could be attributed to cTBS-PFC in either monkey. Importantly, any changes in error rates across cTBS-PFC in both monkeys closely resembled those seen across cTBS-SHAM.

Saccadic Reaction Time. We present the data for saccadic reaction time (RT) in a similar manner, first showing the data recorded before and after cTBS broken down by cTBS location and monkey (Fig. 3A,B), and then by representing the change in RT across cTBS locations (Fig. 3C,D). RT data are only shown for correctly-executed trials. As expected, RT were generally longer for anti- than pro-saccades, although this tendency was much more pronounced for monkey Gr (Fig. 3A) than monkey Bu (Fig.

3B). In Monkey Bu, the general trend is for RT to decrease after cTBS (Fig. 3B); a similar trend was not apparent in Monkey Gr (Fig. 3A).

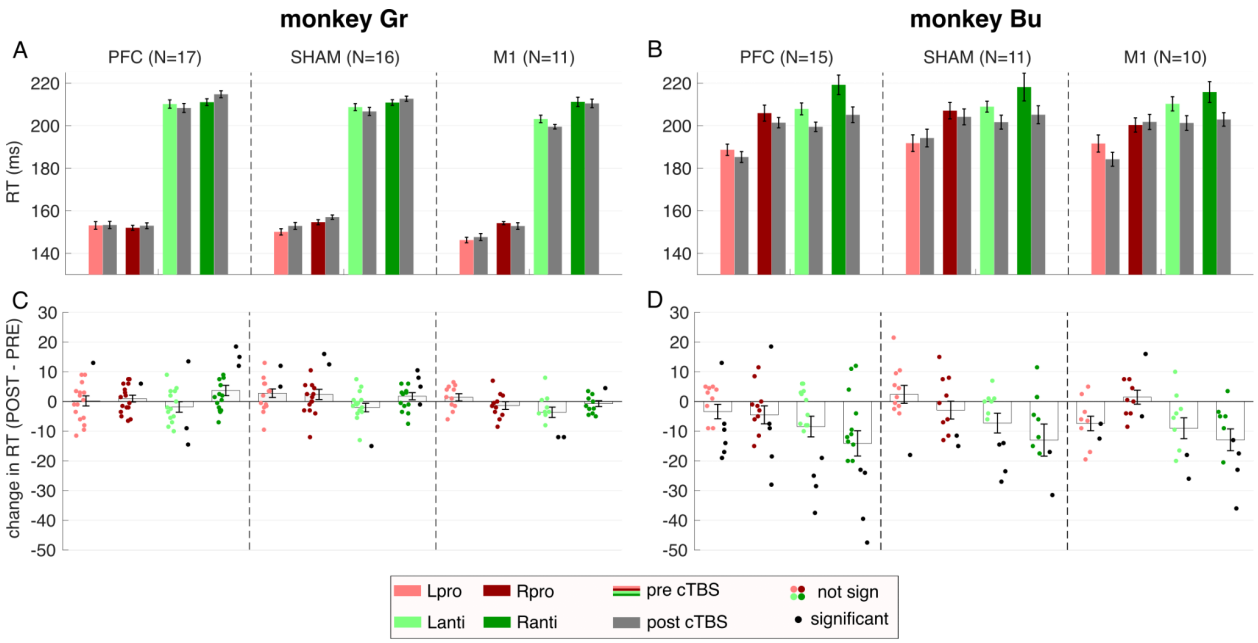

Fig.3 Effects of cTBS on saccadic reaction time (RT). Same general format as Fig. 2. **A,B**. RTs before and after cTBS-delivery for both monkeys, averaged across sessions. **C,D**. RT changes following cTBS delivery, relative to baseline. Black markers shifted to the right of each bar graph indicate individual sessions with significant RT changes for that condition on that day (1-way ANOVA, uncorrected), while red/green markers shifted to the left of each bar graph indicate sessions without significance.

As with error rate, there was no evidence that the change in saccadic reaction time (RT) following cTBS depended on stimulation site. There was no main effect of cTBS location in either monkey (Gr: $F(2) = 1.47$, $p = 0.24$; PFC = 0.8 ms ± 0.9, SHAM = 1.2 ms ± 0.9, M1 = –1.1 ms ± 1.1; Bu: $F(2)=0.19$, $p = 0.83$; PFC = –7.6 ms ± 2.6, SHAM = –5.2 ms ± 3.0, M1 = –7.0 ms ± 3.1). In monkey Gr, we observed a small but significant main effect of saccade direction ($\beta = -1.6$, SE = 0.8, $p_{adj} = 0.049$, 95% CI [0.0, 3.3]), with higher RT change for rightward (1.1 ms ± 0.7) than leftward saccades (–0.5 ms ± 0.7). A significant interaction between saccade direction and saccade type was also found, driven by greater RT change for leftward pro-saccades (1.5 ms ± 0.9) compared to

leftward anti-saccades (–2.5 ms ± 0.9, p_{adj} = 0.005), and by lower RT change for leftward anti-saccades relative to rightward anti-saccades (1.6 ms ± 0.9, p_{adj} = 0.004).

In monkey Bu, there was a significant main effect of saccade type (β = –4.2, SE = 0.7, p < .001, 95% CI [–5.5, –2.9]), with greater RT reduction for anti-saccades (–10.8 ms ± 1.8) compared to pro-saccades (–2.4 ms ± 1.8, p_{adj} < 0.001). A significant interaction between saccade type and saccade direction was also found, reflecting greater RT change for leftward anti-saccades (–8.2 ms ± 2.0) compared to leftward pro-saccades (–2.8 ms ± 2.0, p_{adj} = 0.03). Notably, none of these interaction effects involved cTBS location.

Sessions with significant RT changes across cTBS. Recent studies suggest that the effects of cTBS can vary across days within the same individual, likely due to state-dependent factors (Boucher *et al.*, 2021; Ozdemir *et al.*, 2021). We therefore assessed whether the proportion of sessions with significant within-session RT changes differed by stimulation site. Significant RT changes are indicated by black markers in Fig. 3C–D, which lie above or below the x-axis, representing sessions with increased or decreased averaged RT post-cTBS, respectively (see Table 1 for details).

In monkey Gr, significant RT changes were rare (12%, 14%, and 7% of sessions for cTBS-PFC, SHAM, and M1, respectively), with a trend toward more effects in anti-saccades, but no association with stimulation site (Chi-Square test, $\chi^2(2, N = 176) = 1.38$, p = 0.50). In contrast, monkey Bu showed more frequent RT changes (32%, 23%, and 25% for cTBS-PFC, SHAM, and M1), although though the slightly higher proportion following PFC stimulation did not reach significance ($\chi^2(2, N = 144) = 1.15$, p = 0.56).

Exploring cTBS-induced short-term changes in saccadic RT. Finally, the behavioural effects of cTBS may last for only a few minutes (Huang *et al.*, 2005). Figure 4A&B (top rows) shows the trends of single-trial RTs relative to the time of cTBS delivery ("trial zero"), covering the 200 trials within the PRE- and POST-sessions

	monkey Gr (Fig 3C) *No of sessions sign / ns* *(% sign fractions)*						**monkey Bu** (Fig 3D) *sign / ns* *(% sign fractions)*				
	L-pro	***R-pro***	***L-anti***	***R-anti***	***total***		***L-pro***	***R-pro***	***L-anti***	***R-anti***	***total***
PFC	1 / 16 (6%)	1 / 16 (6%)	3 / 14 (18%)	3 / 14 (18%)	**8 / 60 (12%)**		6 / 9 (40%)	5 / 10 (33%)	4 / 11 (27%)	4 / 11 (27%)	**19 / 41 32%**
SHAM	2 / 14 (13%)	2 / 14 (13%)	1 / 15 (6%)	4 / 12 (25%)	**9 / 55 (14%)**		1 / 10 (9%)	2 / 9 (18%)	4 / 7 (36%)	3 / 8 (27%)	**10 / 34 23%**
M1	0 / 11 (0%)	0 / 11 (0%)	2 / 9 (18%)	1 / 10 (9%)	**3 / 41 (7%)**		2 / 8 (20%)	2 / 8 (20%)	2 / 8 (20%)	4 / 6 (40%)	**10 / 30 25%**

Table 1. Proportion of sessions showing significant or non-significant changes in saccadic reaction time (RT) following cTBS, along with corresponding rounded percentages of significant sessions.

(recall that trial types were pseudo-randomly interleaved, thus there were 50 trials of each type before and after cTBS; the colored lines represent data from the three different cTBS locations). For both monkeys, RTs tended to be shorter immediately after cTBS delivery, regardless of cTBS location. These changes were smaller for monkey Gr (ranging around -5ms across conditions, Fig 4A, top row) than monkey Bu (ranging around -20ms, Fig 4B, top row). Further, RTs tended to be more stable through time in monkey Gr, whereas RTs in monkey Bu tended to increase through both the PRE-cTBS and POST-cTBS intervals, perhaps due to decreasing motivation. Such increasing RTs through time are apparent for all cTBS locations, and all trial types. To analyze short-term effects, we examined the distribution of RTs immediately before or after cTBS, only including 25 trials of each condition (opaque grey boxes in the upper row of subplots in Fig. 4). At the rate of trial delivery and performance, each of these grey boxes span ~10 minutes of data.

Figure 4 (bottom rows) shows individual RTs from the +/- 25 trials surrounding cTBS delivery, with light and dark colors indicating trials before and after stimulation, respectively, across all conditions. To analyze any potential short-term effect of cTBS location on saccadic RT, we again employed a linear mixed model, with the factors of cTBS-location (cTBS-PFC, -SHAM, -M1), trial direction (left, right), trial type (pro, anti), and block (pre- and post-cTBS), with individual sessions as random factor. Saccadic

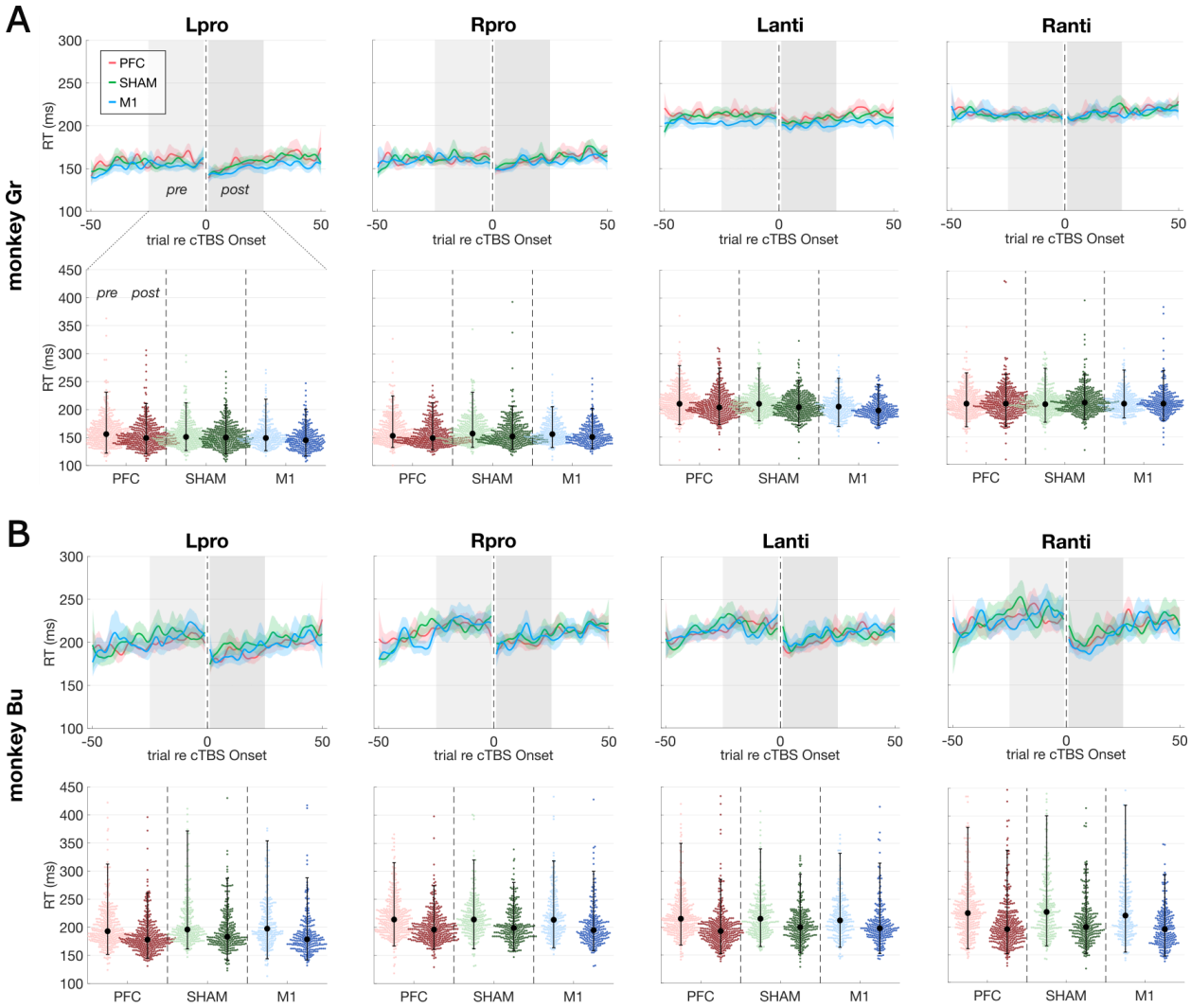

Fig.4 Short-term effects of cTBS on reaction time. Top row (A,B): RT trends over time relative to cTBS delivery (trial 0), shown as mean ± 95% CI across all sessions and cTBS locations (colors), for monkey Gr (A) and monkey Bu (B). Shaded grey areas demarcate the 25 trials before (light) and after (dark grey) cTBS. Bottom row (A,B): Colored dots represent individual RTs within the pre- and post-cTBS windows, with light and dark shades indicating trials before and after cTBS, respectively. Large black dots and error bars show the median and 95th percentile range.

reaction times exhibited a trend to be faster in the post-cTBS blocks compared to the pre-cTBS block in both monkeys (Gr: $F(1) = 59$, $p < 0.001$; Bu: $F(1) = 452$, $p < 0.001$), regardless of stimulation site or saccade condition. Since our primary focus was on site-specific modulation, we examined interaction terms involving cTBS target and block, none of which were significant (Monkey Gr: cTBS target x block: $F(2) = 1.1$, $p = 0.34$; cTBS target x block x direction: $F(2) = 0.01$, $p = 0.99$; cTBS target x block x type: $F(2) = 1.05$, $p = 0.35$; cTBS target x block x direction x type: $F(2) = 0.88$, $p = 0.41$;

monkey Bu: cTBS target x block: $F(2) = 0.9$, $p = 0.41$; cTBS target x block x direction: $F(2) = 0.69$, $p = 0.50$; cTBS target x block x type: $F(2) = 0.54$, $p = 0.58$; cTBS target x block x direction x type: $F(2) = 2.54$, $p = 0.08$). Although post-cTBS RTs were consistently faster than pre-cTBS RTs, there was no evidence of a significant site-specific modulation of this effect.

In summary, we conducted a thorough analysis of the change in RTs across cTBS location, analyzing average changes in RT, the proportion of significant within-session changes in RT, and the time course of RTs. We did not find any evidence that changes in RT could be specifically attributed to cTBS-PFC.

Saccadic peak velocity. As for reaction times, we analyzed the change in average peak velocity across cTBS conditions (Fig. 5C, D). As expected anti-saccades showed slower peak velocities than the more congruent pro-saccades, but with overall relatively small changes in both monkeys. In monkey Bu (Fig. 5D), we found no evidence that peak velocity changes varied as a function of any factor, including cTBS location ($F(2) =0.49$, $p = 0.62$). The mean change in peak velocity was as follows: cTBS-PFC = 8.5deg/s ± 5.2, cTBS-SHAM = 6.1deg/s ± 6.0, cTBS-M1 = 0.4deg/s ± 6.4. In monkey Gr, we observed a significant effect of cTBS location ($p = 0.05$). Post-hoc analyses revealed that this effect was primarily driven by a significant difference between the two control conditions, cTBS-SHAM and cTBS-M1 ($p_{adj} = 0.049$), with cTBS-SHAM showing a change of -12.5deg/s ± 3.9 (95% CI [-20.3, -4.6]) and cTBS-M1 a change of 2.8deg/s ± 4.7 (CI [-6.7, 12.2]). The change in peak velocity for either control condition did not differ significantly from that observed for cTBS-PFC. Additionally, in monkey Gr, we found main effects for saccade type ($p_{adj} = 0.001$, pro = 1.1deg/s ± 2.8, anti = -10.4deg/s ± 2.8) and saccade direction ($p_{adj} = 0.001$, left = 1.8deg/s ± 2.8, right = -11.1deg/s ± 2.8), as well as an interaction effect between saccade type and direction. Significant differences were observed between left- and rightward anti-saccades ($p_{adj} < 0.001$, left-anti = 0.9deg/s ± 3.6, right-anti = -21.7deg/s ± 3.6) and between rightward pro- and anti-saccades ($p_{adj} < 0.001$, right-pro = -0.5deg/s ± 3.6, right-anti = -21.7deg/s ± 3.6).

In summary, although peak saccade velocity in monkey Gr was significantly influenced by saccade type, direction, and cTBS location, we found no specific evidence that the change in peak velocity was selectively driven by cTBS-PFC.

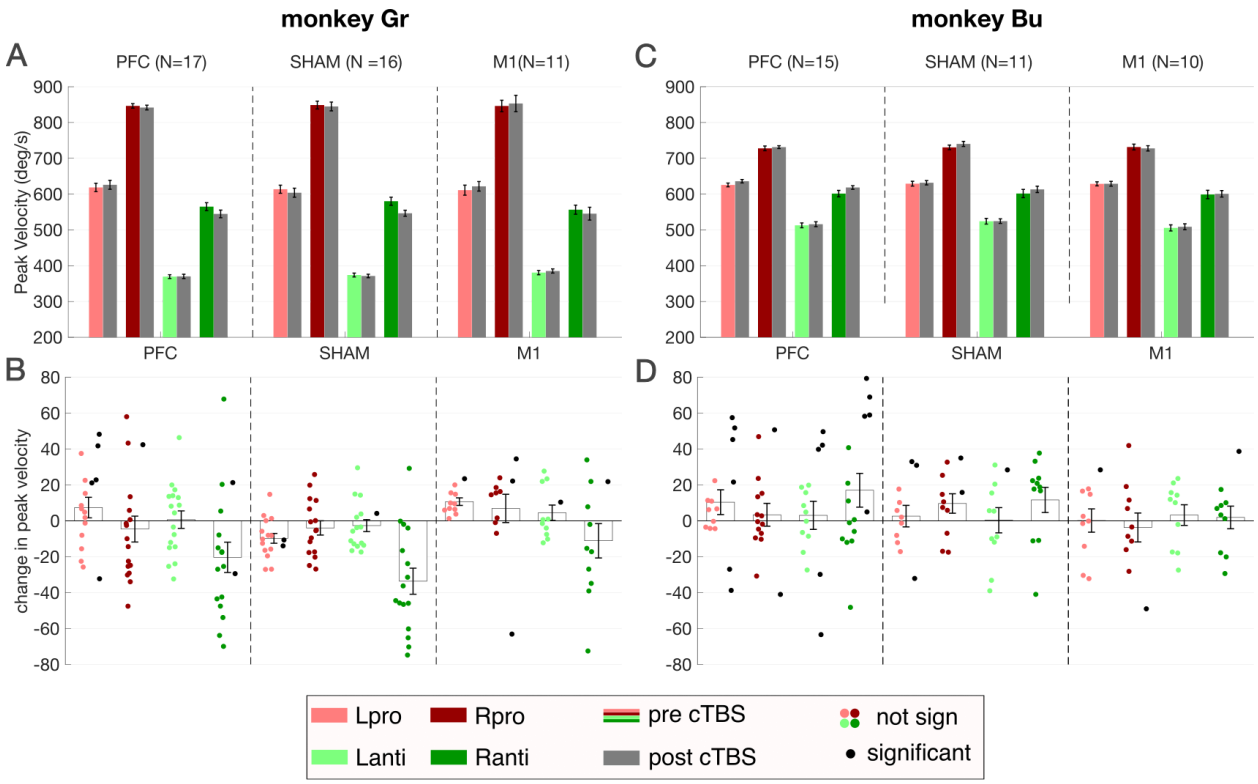

Fig.5 Effects of cTBS on saccadic peak velocity. Same general format as Figs. 2 and 3. **A,B**. Peak velocities before and after cTBS-delivery or both monkeys, averaged across sessions. **C,D**. Change in peak velocity following cTBS delivery, relative to baseline. Black or coloured markers shifted to the right or left denote individual sessions with significant on non-significant changes in peak velocity, respectively (1-way ANOVA, uncorrected)

Analyses of neural spiking activity

***D*escription of functional tuning before cTBS.** Despite the absence of a behavioral effect attributable to cTBS-PFC, cTBS-PFC may influence neural activity in more subtle ways, perhaps below the threshold required for a behavioral change or by inducing both excitatory and inhibitory effects. To explore this, we analyzed neural activity from Utah arrays chronically implanted in the frontal cortex contralateral to the cTBS site. Our analysis assesses changes in neural activity induced by cTBS within a session,

comparing activity relative to the baseline preceding cTBS. We recorded 3,921 single units from 44 sessions in monkey Gr (averaging 89 units per session) and 873 units from 37 sessions in monkey Br (averaging 24 units per session). Given the stability of unit recordings over time with Utah arrays (Sponheim *et al.*, 2021), many units were likely recorded across multiple sessions.

A large proportion of units exhibited task modulation, and we focused on neural activity during: (1) the "rule epoch" following rule instruction, (2) the "visual response epoch" shortly after target onset, and (3) the "peri-saccade epoch" around saccade execution. Figure 6A-C illustrates three example neurons exhibiting tuned activity in these three time periods before cTBS, with the shaded areas illustrating the analysis interval. The neuron in Figure 6A exhibited higher activity for anti-saccades (green) compared to pro-saccades (red), which persisted even after removal of the instruction cue, consistent with previous reports of rule maintenance in PFC (Wallis, Anderson and Miller, 2001; Everling and DeSouza, 2005). The neuron in Figure 6B responded more strongly to visual targets in the contralateral field, with essentially identical responses on R-pro and L-anti trials. The neuron in Figure 6C exhibited higher activity before rightward (contralateral) saccades, with similar increases for R-pro and R-anti trials.

Figure 6D-F shows population tuning properties for all neurons recorded in the two monkeys, based on their activity in these epochs (dark points indicate neurons where activity was significantly modulated during the respective epoch using a 1-way ANOVA, $p<0.01$). Of the 3979 neurons recorded in monkey Gr (left column in Fig. 6D-F), 6% of neurons exhibited rule-tuning (4% for anti-saccades), 32% exhibited visual tuning (21% for contralateral targets), and 36% were tuned for saccade direction (20% for contralateral saccades). Out of the 873 neurons recorded in monkey Bu (Fig. 6D-F, right), only 9 units (1%) were rule-tuned, 13% exhibited visual tuning (10% for contralateral targets), and 15% were tuned for saccade direction (8% for contralateral saccades). These preferences for contralateral tuning to visual targets and more balanced contra- vs- ipsilateral tuning to saccade direction resembles previous findings in area 8Ar (Bullock et al., 2017).

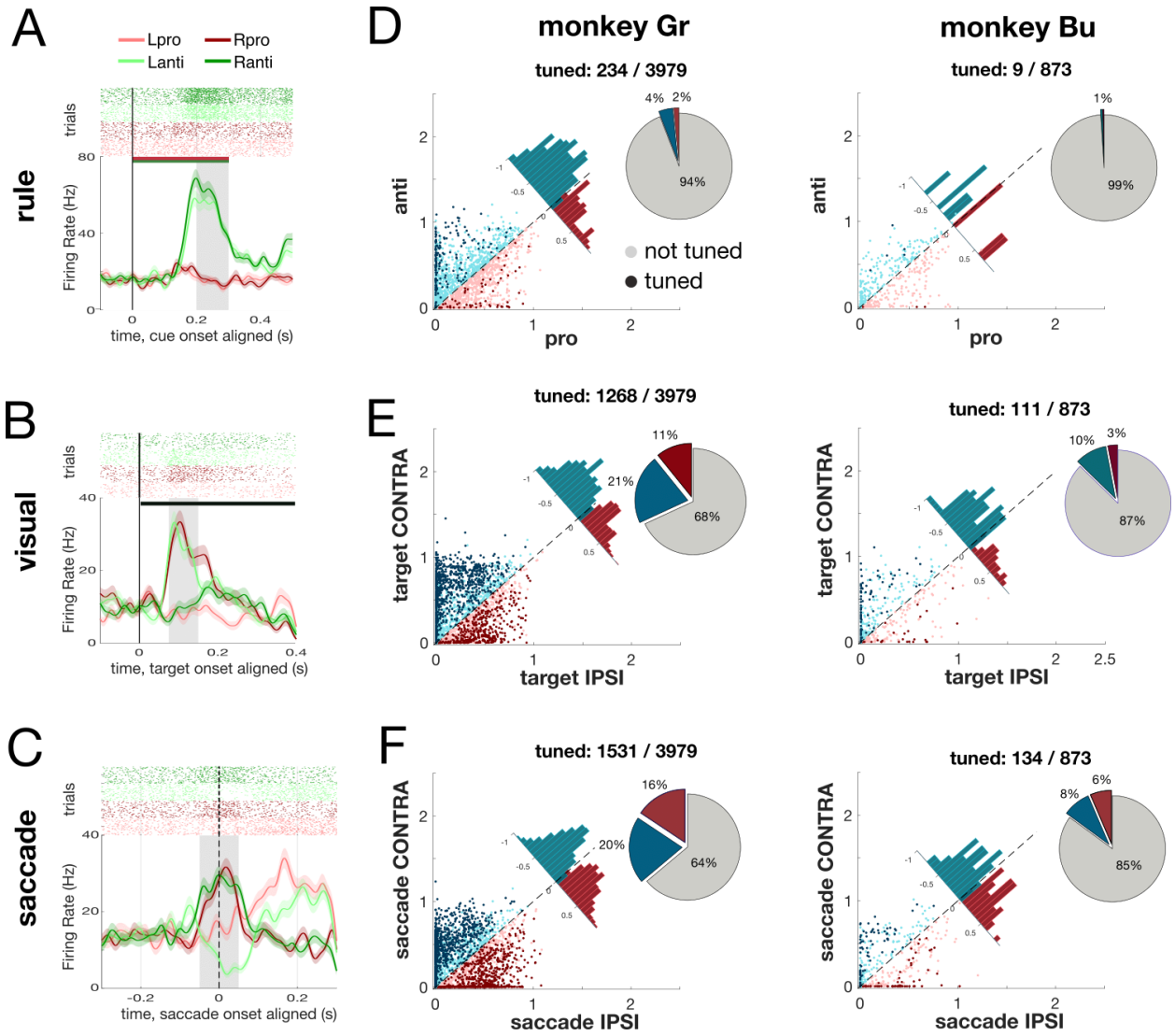

Figure 6. Task specific activity: single unit examples and population tuning. A–C Three examples of task-modulated neurons recorded in area 8Ar, showing a unit preferentially active for anti-saccades (A, aligned to cue onset, horizontal bars depict time of rule instructions), a unit with a visual response to contralateral targets (B, R-pro & L-anti, aligned to target onset), and a unit exhibiting greater activity before contralateral saccades (C, R-pro & R-anti, aligned to saccade onset). Shaded grey areas denote the analysis epochs. **D–F** Population tuning across both monkeys (monkey Gr, left; monkey Bu, right), showing the distribution of tuning directions and the percentage of neurons significantly modulated during each epoch (D: rule epoch, E: visual response epoch, F: saccade epoch). Points represent normalized firing rates of individual neurons (in arbitrary units), with darker shades indicating a significant modulation (1-way-ANOVA, $p<0.01$), and colors denoting tuning direction. Histograms display the distribution of tuning directions for significantly modulated units, while pie charts indicate the proportion of tuned units relative to the total recorded population in each monkey.

Assessment of changes in task-related activity over time. Neural activity in the PFC can vary during a session due to fluctuations in slow-varying factors like attention, arousal, and motivation (Cowley *et al.*, 2020). Given our blocked design, such longer-timescale variations may mask any changes induced by cTBS. Thus, we first examined changes in task-related activity across the entire session, and used this to define the interval over which we analyzed changes induced by cTBS. Figure 7 shows the average activity of significantly task-modulated units in each epoch, aligned to the time of cTBS delivery (trial 0). In both monkeys, we generally observed a gradual decrease in neural activity, particularly in the visual (Fig. 7B, E) and saccade (Fig 7C, F) epochs; the exception is the general increase in the activity of neurons encoding the anti-saccade rule in monkey Gr (Fig. 7A, right panel). Over the timeframe of the 200 trials before and after cTBS, these slow fluctuations could change normalized neural activity by ~10-20%, regardless of cTBS location. To reduce the influence of these non-cTBS-specific, time-dependent changes while preserving sufficient trial numbers, we focused subsequent statistical analyses on the 25 trials immediately before and after cTBS (highlighted in grey in Fig. 7; these intervals span ~10 minutes each). We also conducted the same analysis across the full set of trials (not shown), but this did not provide any additional insights beyond what is reported below.

Population analysis of cTBS effects on spike rates. Figure 8 shows the change in average spike rate across cTBS for every neuron that exhibited significant tuning during the various epochs of the task. Given that cTBS was delivered to the other hemisphere, contralateral disinhibition predicted increased neural activity following cTBS-PFC, i.e., the red distributions in Fig. 8 should shift upward. As with the behavioral analyses, we applied linear mixed models to test the effects of cTBS location (PFC, SHAM, M1) and trial type (pro- vs. anti-saccades), and included saccade direction (left vs right) for the visual and saccade epochs. Unit ID was included as a random factor. For clarity and brevity, we focus on significant results and main or interaction effects of cTBS location.

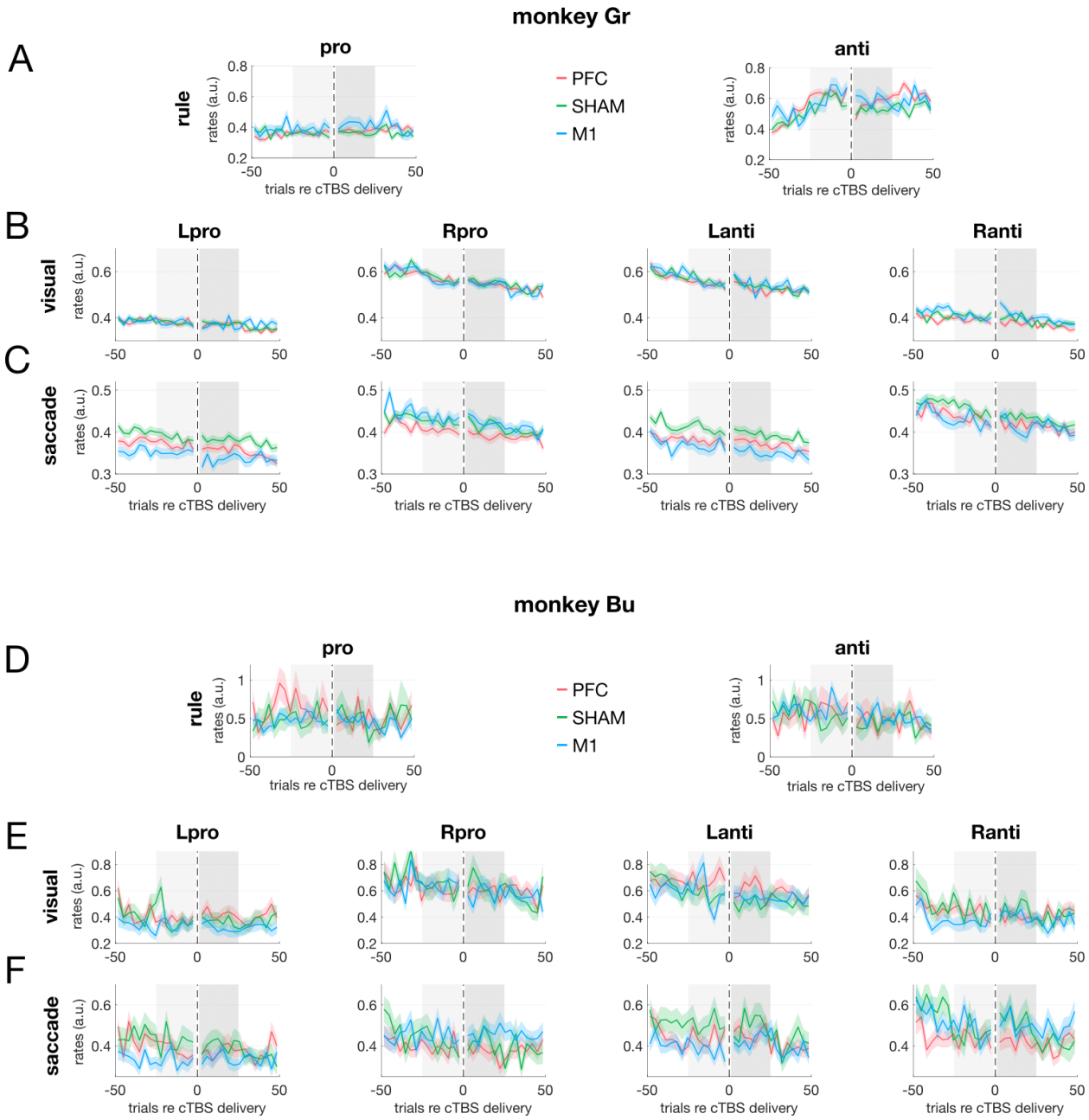

Fig.7 Normalized spiking activity of task modulated neurons over time. Average normalized spike rates for all significantly task-modulated units, aligned to the time of cTBS delivery (trial 0), shown separately for monkey Gr (A–C) and monkey Bu (D–F). Each row corresponds to a different task epoch: rule (A, D), visual (B, E), and saccade (C, F). For the rule epoch, neural activity is grouped by saccade type (pro vs. anti); for the visual and saccade epochs, all four task conditions are displayed. Line colors indicate cTBS location (PFC, SHAM, M1), shaded colored areas represent SEM. Grey shaded areas indicate the time windows used for subsequent statistical analyses of cTBS-induced effects. Y-axis scales (in arbitrary units) vary between epochs and monkeys to best illustrate condition-specific trends.

In monkey Gr, neurons tuned during the rule epoch (Fig 8A) showed a significant main effect of saccade type on rate change (b = –0.07, SE = 0.018), t(693) = –3.69, p<0.001, with firing rates going down after cTBS more for anti-saccades than pro-saccades (Fig. 7A). However, there was no significant main effect of cTBS location (F(2)=0.58, p=0.56), nor any significant interaction terms that included cTBS location. During the visual epoch (Fig 8B), no significant rate changes were observed across factors, although the effect of cTBS location approached significance (F(2)=2.83, p=0.06). For the saccade epoch, a marginally significant interaction between cTBS location and saccade type (F(2)=3.27, p=0.038) did not withstand Bonferroni correction. In monkey Bu, no effects were found in the rule epoch (Fig 8D; F(2)=0.91, p=0.41), but we note the very small number of task-modulated units (n=9). During the visual epoch (Fig 8E), we observed a significant interaction between cTBS location and saccade type (F(2)=9.52, p<0.001), but note that this effect seems to be primarily driven by the decreases seen after cTBS-M1 (mean = –0.11±0.04) compared to the small increases in activity after cTBS-PFC (p_{adj}<0.01, mean = 0.06±0.03) or SHAM (p_{adj} = 0.03, mean=0.06±0.04). No significant effects were found in the saccade epoch (Fig 8F; F(2)=2.05, p=0.13).

In summary, cTBS appeared to induce only minimal effects in the population of task-modulated activity, with no consistent or strong influence of cTBS location. Importantly, we found no evidence of disinhibition following cTBS-PFC.

Session-by-session analysis of cTBS effects on spike rates. Finally, we analyzed the possibility that the neural effects of cTBS may change across days, perhaps being more effective on some days than others. We therefore repeated the above analyses after averaging the changes in spike rate across cTBS across all units recorded on a given day (Figure 9). In monkey Gr, we observed no evidence of an effect of cTBS location on neural activity in the rule epoch (Fig. 9A; F(2)=0.71, p=0.50) or saccade epoch (Fig. 9C; F(1)=2.51, p=0.12). We observed a significant interaction between saccade type and cTBS location during the visual epoch (Fig. 9B; F(2)=5.86, p=0.004), which was driven by a greater reduction in activity accompanying anti-saccades in cTBS-SHAM (mean = –0.013 ± 0.003) compared to cTBS-PFC (mean

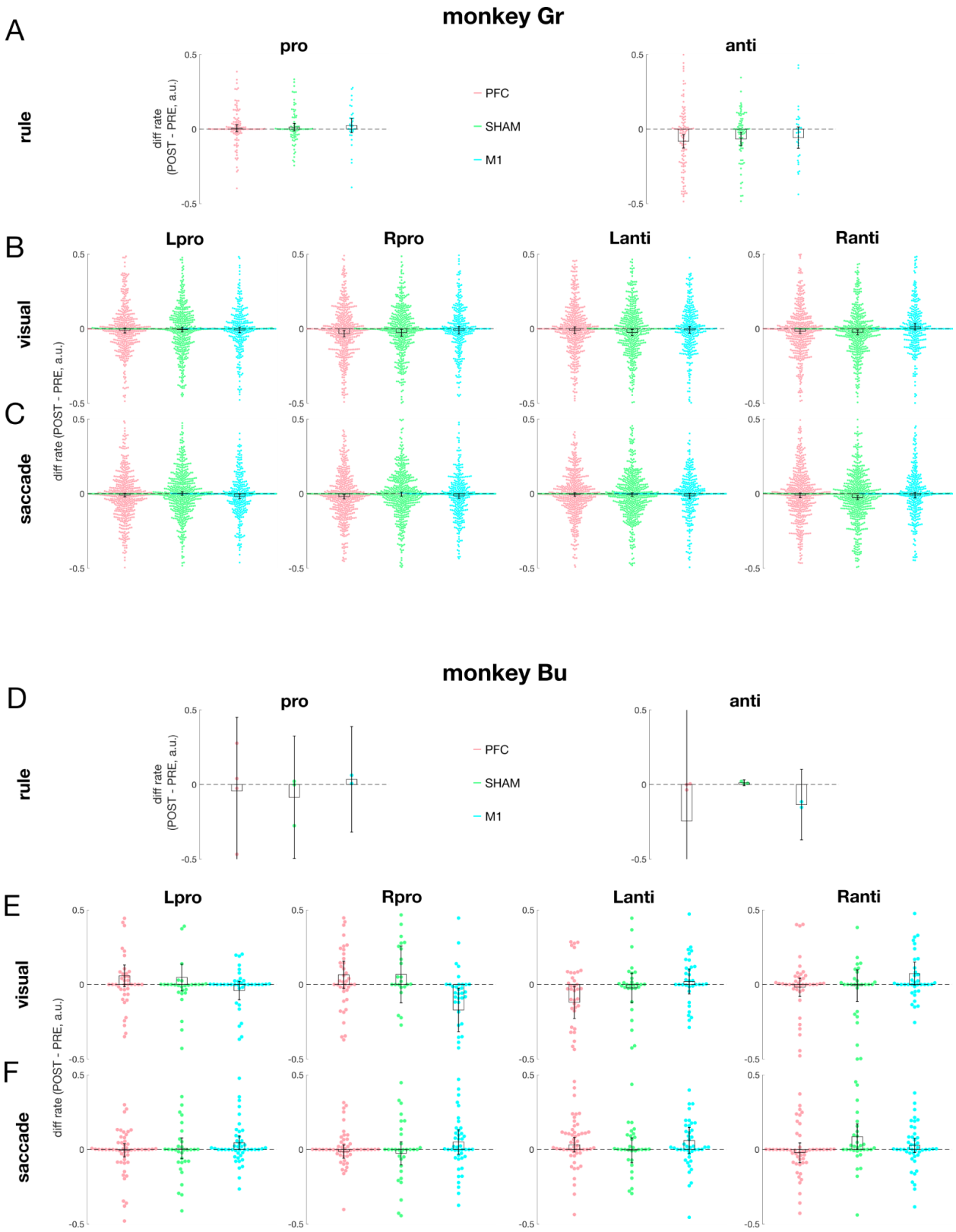

Fig. 8. Effects of cTBS on normalized spike rates of individual neurons. Differences in spiking (post–pre cTBS, in arbitrary units) for all significantly task-modulated neurons in each epoch, shown for

monkey Gr (A–C) and monkey Bu (D–F). Rows correspond to task epochs: rule (A, D), visual (B, E), and saccade (C, F). For the rule epoch, data are grouped by saccade type (pro vs. anti); for the visual and saccade epochs, all four task conditions are shown. Data points represent rate changes of individual neurons (positive values denote an increase in activity after cTBS); colors indicate cTBS location (PFC, SHAM, M1). Bars show group medians; black error bars represent SEM.

= 0.002 ± 0.003, p_{adj}=0.03) or cTBS-M1 (mean = 0.003 ± 0.004, p_{adj}=0.04). For the saccade epoch (Fig 9C), the interaction between cTBS location and saccade type was again significant (F(2)=3.49, p=0.032), though follow-up contrasts were non-significant (all ps > 0.08). In monkey Bu, analysis of spiking activity in the rule epoch (Fig 9D) showed no evidence of a significant effect, but we note the limited data (see previous section). Analysis for the visual epoch (Fig 9E) revealed a significant interaction between cTBS location and saccade type (F(2)=5.37, p=0.007), with a significant fixed-effect parameter for M1-PFC x anti–pro (β = –0.12, SE=0.14, p=0.003), but not for SHAM-PFC (β = 0.015, SE=0.07, p=0.80). Again, post-hoc comparisons did not reveal significant pairwise differences (all ps > 0.23). No significant effects were observed in the saccade epoch (Fig 9F; all ps > 0.1).

Taken together, analyses across both individual neurons and session-level averages revealed no evidence for any consistent influence of cTBS to the PFC on spiking activity in the contralateral PFC. While we observed some significant interaction effects during the visual and saccade epochs, these effects were not consistent across monkeys, generally did not survive corrections for multiple comparisons, and varied considerably in both absolute magnitude and directionality. Thus, we did not see any evidence for disinhibition following cTBS-PFC when compared to the cTBS-SHAM and cTBS-M1 controls. Broadly speaking, the absence of disinhibitory effects aligns with the lack of any behavioural changes after cTBS.

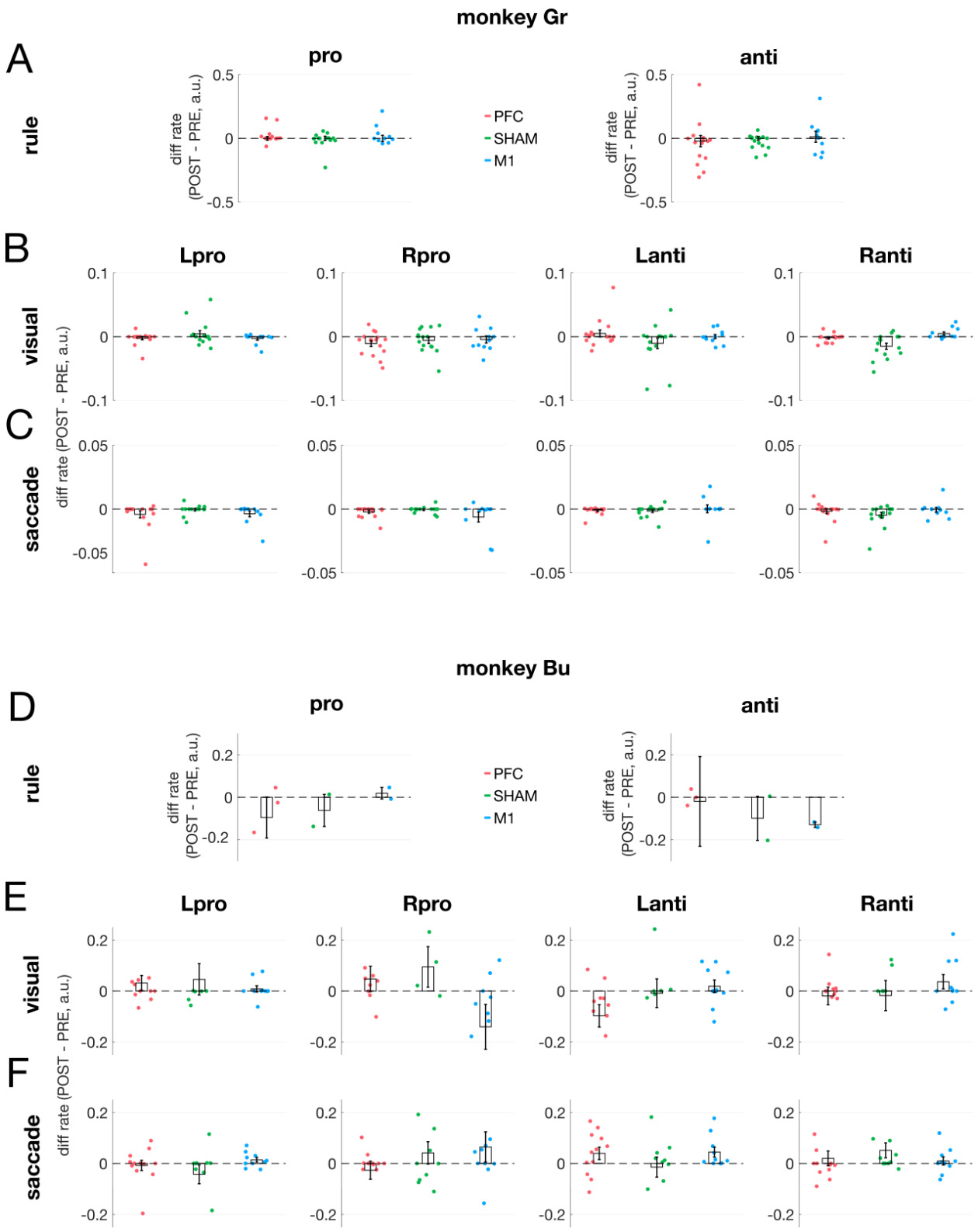

Fig. 9. Effects of cTBS on normalized spike rates averaged within sessions. Same format as Fig 8, except that each data point shows the change in spiking activity of significantly task-modulated, averaged within a given session (i.e., one data point per session containing tuned units).

Discussion

We investigated the behavioural and neural effects of delivering cTBS to the prefrontal cortex of two rhesus macaques performing an oculomotor task. Our study tested the hypothesis that cTBS will inhibit the PFC, and disinhibit the mirroring, contralateral PFC. We did not find any reliable behavioral or neural evidence consistent with this hypothesis, as any changes across cTBS to the PFC were equally likely when applying cTBS to either M1 or to the air. These are effectively negative results, and we report them in the context of recent reviews that have emphasized the importance of reporting such results for the field (Héroux, Taylor and Gandevia, 2015; Ziemann and Siebner, 2015). Work in animal models, and NHPs in particular, do not afford the opportunity for extensive pilots, and in this Discussion we will consider a number of methodological choices that, in retrospect, may have been suboptimal. Overall, our results contribute to a growing series of studies that question the fundamental assumptions of notion of cTBS-mediated inhibition and consequent disinhibition of callosal targets, and emphasize the challenges associated with assessing changes in neural activity across intermediate timescales given the known fluctuations in PFC activity.

Choice of behavioural task, and rationale for using a repetitive mode of TMS

We trained our animals to perform an inter-mixed pro- and anti-saccade task that required them to first encode and then remember this instruction in order to correctly complete the trial following peripheral target presentation. The memory component increases the complexity of the task, which is reflected in the elevated pro-saccade error rate particularly in monkey Bu (Fig. 2B) compared to when the instruction cue persists for the entire trial (Everling, Dorris and Munoz, 1998). We chose this task given the excellent understanding of the neural correlates of task performance (Munoz and Everling, 2004), and since anti-saccades have been used in other studies delivering TMS to the FEF in macaques (Valero-Cabre *et al.*, 2012) and humans (Olk *et al.*, 2006; Beynel *et al.*, 2014; Cameron, Riddle and D'Esposito, 2015). Our choice of task is validated by PFC activity reflecting both rule maintenance (Wallis, Anderson and Miller, 2001; Everling and DeSouza, 2005), and the visuo-motor transformation (Bullock *et al.*, 2017; Khanna, Scott and Smith, 2020). The interpretation of our results are bolstered

through comparisons to results in similar tasks that modulate PFC activity through other means to change behaviour and/or neural activity (Wegener, Johnston and Everling, 2008; Phillips, Johnston and Everling, 2011; Pouget *et al.*, 2020).

Another common task used to assess how a given intervention may change neural activity or behaviour is the stimulus-onset asynchrony (SOA) task, which staggers the presentation time of diametrically-opposed targets (Balan *et al.*, 2017; Adam, Johnston and Everling, 2019; Kubanek *et al.*, 2020). The influence of a given intervention can be assessed by shifts in the timing at which the subject would look to either target with equal likelihood. This is a simpler task than the one we employed, and behavioural shifts in the point of equal selection can often be explained by the changes in RTs to look to single left or right targets (Rincon-Gonzalez *et al.*, 2016). Given the unchanged RTs of either pro- or anti-saccades, it seems unlikely that behavioural effects would have been observed in the SOA task.

A rTMS study necessitates blocked “before-vs-after” analyses. The application of cTBS clearly influenced multiple aspects of oculomotor behaviour and PFC activity, but this influence was the same regardless of cTBS target. Simply delivering cTBS likely influences the animal’s arousal, which temporarily shortens RTs (Fig. 4) and elevates the visual and motor responses (Fig. 7). The dynamics of such changes complicate the identification of effects attributable to cTBS-PFC, as any such changes would have to ride on top of the already substantial changes induced by non-specific arousal. Other groups have reported behavioral and neural changes in NHPs across rTMS that exceed that attributable to non-specific arousal (Romero *et al.*, 2019, 2022), but we simply did not see this here. Further, rTMS protocols may be more effective when the targeted area is actively engaged in a task (for a review, see Beynel *et al.*, 2019); while intriguing, the effectiveness and directionality of this approach has not been sufficiently established to warrant the additional training required for experimental animals.

Finally, teaching animals the pro-/anti- saccade rule required progressive stages of training. A nuance in the current dataset is that monkey Bu had a longer training history

than monkey Gr before the start of data collection, and in both monkeys the cTBS-M1 sessions were acquired after a substantial number of cTBS-PFC and -SHAM sessions (see Methods). This difference in training history likely explains why monkey Gr's anti-saccade error rates were generally lower in the M1 sessions compared to the PFC and SHAM sessions (Fig 2). The importance of training history is also apparent in the work by Gerits and colleagues (2011), wherein saccadic RTs decreased considerably by the time data from cTBS-M1 was collected. But even if this factor is included, the lack of any difference between data from cTBS-PFC vs cTBS-SHAM in monkey Gr persists.

Choice of TMS parameters and controls

rTMS protocol. We decided to use cTBS rather than 1-Hz rTMS for both pragmatic and theoretical reasons. Delivery of 600 cTBS pulses requires only ~40s, whereas an equivalent number of pulses at 1-Hz requires 10 minutes. Given the before-vs-after nature of our analyses, we opted for a briefer time for rTMS delivery. There is also evidence for superior effects of cTBS than 1-Hz rTMS, although such effects may not last as long (Di Lazzaro *et al.*, 2010). There is also emerging evidence that delivering more rTMS pulses in a single bout of cTBS results in longer lasting effects (Wischnewski and Schutter, 2015), but doing so would have overheated the TMS coil.

Interleaving cTBS sessions Our decision to interleave cTBS-PFC or cTBS-M1 sessions with cTBS-SHAM days was motivated by a desire to avoid the potential of cumulative effects of cTBS (see Valero-Cabré, Pascual-Leone and Rushmore, 2008). Separating sessions where cTBS is delivered to the brain by at least 48 hours permits within-session analyses unconfounded by the history of what was delivered the day before. This interleaved approach may have decreased the likelihood of seeing cTBS effects, particularly given recent trends advocating for more TMS pulses within a given day, and across sequential days (Lefaucheur *et al.*, 2014, 2020). The decision to interleave cTBS sessions is also influenced by the limited number of NHPs, the potential confounds with training history (see above), and the possibility of device failure or decreasing yields over time inherent with chronically-implanted recording arrays. It is also possible that cTBS effects would have been realized had we delivered multiple

bouts of cTBS on a given day (e.g., 1200 pulses total; (Gerits *et al.*, 2011; Balan *et al.*, 2017)), although we note that work in macaques has reported an influence of cTBS on brain activity and behaviour with only 300 individual pulses during 20 s of cTBS (Merken *et al.*, 2021; Romero *et al.*, 2022).

TMS intensity. In humans, a typical pulse intensity for cTBS to M1 is 80% of resting motor threshold (Di Lazzaro *et al.*, 2005; Huang *et al.*, 2005; for a review see Fitzgerald, Fountain and Daskalakis, 2006). The absence of any effects in our study contrasts with reports of cTBS changing grasping behaviour and neural excitability in the macaque parietal cortex (Merken *et al.*, 2021; Romero *et al.*, 2022), and on saccade behaviour and intra- and inter-hemispheric functional connectivity in the macaque FEF (Gerits *et al.*, 2011; Balan *et al.*, 2017). These studies also delivered cTBS at an intensity of ~80% of resting motor threshold, whereas we used higher pulse intensities above the resting motor threshold to resemble that used in the DLPFC for treatment of intractable depression (Lefaucheur *et al.*, 2014; Van Rooij *et al.*, 2024). Dose–response relationships in TMS are often nonlinear (Bergmann and Hartwigsen, 2020), and the tradeoff between pulse intensity and effect focality is particularly pertinent in smaller brains, but we view it as unlikely that the absence of neural or behavioural effects observed here relate the higher pulse intensity.

We are also confident that cTBS of the PFC or M1 influenced brain activity. While we did not record neural activity in the PFC targeted by cTBS, we reconfirmed every day that single-pulse TMS-M1 or -PFC evoked small contralateral thumb twitches (with the latter being more infrequent and smaller, consistent with a degree of focality). Many aspects of our implant design and pulse intensity resemble that used in our previous study, wherein single pulses of TMS over a widespread area of frontal cortex, including the PFC location we targeted, induced a feed-forward neck muscle response (Gu and Corneil, 2014). In retrospect, obtaining such objective markers to single-pulse TMS-PFC would have provided further insights about the effects of cTBS. For example, Romero and colleagues (2022) showed that cTBS to the parietal cortex reduced the neural response to single-pulse TMS. Despite such a reduction, cTBS to the parietal cortex did

not influence the feedforward response to a visual stimulus, paralleling our finding of the lack of any influence of cTBS-PFC on the visual response in the contralateral hemisphere.

Choice of controls. We included both a SHAM and a brain (M1) control to control for non-specific effects of cTBS delivery, including tactile and auditory sensations, and changes in arousal. While the PFC and M1 stimulation sites were separated by ~8mm, distinct neck muscle responses can be evoked from these locations (Gu and Corneil, 2014). However, given that our stimulation intensity is above resting motor threshold, is it possible that both cTBS-PFC and cTBS-M1 influenced the oculomotor network? Our results provide no evidence for this, as the effects of either cTBS-PFC or cTBS-M1 did not reliably stand out from those induced by cTBS-SHAM. Alternatively, an intensity control could have been employed to investigate potential dose-dependent effects, but in retrospect it is unlikely that an intensity control would have provided additional insights, given the absence of clear differences between cTBS applied to the PFC, M1, and SHAM conditions.

Assessment window for behavioural and neural effects. Is it possible that our analyses examined intervals that were either too soon or too late after cTBS? The original report showed that the decrease in cortical excitability following cTBS peaks ~5-10 minutes later (Huang *et al.*, 2005), but decreases certainly begin within the first few minutes. More recent reviews have focused on the duration of such effects on neural excitability, which exceed 20 minutes or more depending on the number of cTBS pulses delivered (Thut and Pascual-Leone, 2010; Wischnewski and Schutter, 2015). In the macaque, the work from the Janssen lab (after 300 pulses of cTBS) show more variability in the timing of peak effects after cTBS to the parietal cortex, with such effects peaking ~20-30 min after cTBS (Merken *et al.*, 2021; Romero *et al.*, 2022). However, even in this work, reliable changes in behaviour or neural excitability begin to appear soon after cTBS, even if the peak effect is delayed. Our presentation of saccadic RT (Fig. 4) or neural activity (Fig. 7) through time emphasizes that the time-dependent effects were common to all cTBS conditions. Finally, we note that mechanisms often

invoked to explain the delayed nature of the effects of cTBS, such as a delayed increase in GABA levels (Stagg *et al.*, 2009) in the stimulated area and an associated decrease in the contralesional hemisphere (Matsuta *et al.*, 2022) should have altered saccade behaviour, given the effects of delivery of GABA agonists or antagonists to the FEF (Dias, Kiesau and Segraves, 1995). We found no evidence of this in our data.

Further technical considerations. The TMS coil used for this study has been widely employed in previous NHP research (e.g., Amaya *et al.*, 2010; Gerits *et al.*, 2011; Valero-Cabre *et al.*, 2012; Gu and Corneil, 2014; Romero *et al.*, 2019, 2022; Merken *et al.*, 2021). It is big enough for efficient delivery of cTBS while small enough given the spatial constraints imposed by cranial implants. The cranial implant was optimized to avoid field distortion and minimize the distance from coil to skull by incorporating a thin acrylic layer (~5 mm; for details, see (Gu and Corneil, 2014)). Precise and repeatable coil placement was ensured via neuronavigation, which was further confirmed via the consistency of the evoked thumb twitches from single-pulse TMS-M1 at the start of every session; coil orientation has been shown to be a relatively negligible factor for this type of coil (Alekseichuk *et al.*, 2019). Overall, it is unlikely that any of these technical considerations explained the lack of cTBS-PFC effects. Finally, we delivered biphasic pulses, while some evidence is showing that monophasic pulses induce stronger and longer-lasting effects (Tings *et al.*, 2005; De Lima-Pardini *et al.*, 2023); this may be a parameter to modify in future studies.

No influence of cTBS-PFC on spiking activity in the mirroring, contralateral PFC

The effects of non-invasive brain stimulation are not limited to the targeted area, and the possibility that cTBS-mediated inhibition can be used to induce balanced or compensatory excitation in the mirroring, contralateral target has clear value for basic and clinical research. One message of our manuscript is the lack of evidence for this in terms of task-relevant spiking activity in the contralateral PFC. This absence is all the more surprising considering findings in macaques that show that very similar cTBS protocols can alter the excitability of the targeted area to single-pulse TMS in the parietal cortex (Romero *et al.*, 2019), and functional connectivity in the frontal cortex,

including to the mirroring, contralateral target (Balan *et al.*, 2017). In our study, cTBS-PFC may not have induced a strong enough perturbation for changes in task-related neural activity to stand out from the already substantial fluctuations in neural activity in this area. Further, there may well be other perhaps more sensitive measures of neural activity (e.g., local field potentials, and/or spike-field coherence) that do change with cTBS-PFC; such measures will be explored in a future manuscript.

PFC may also not be an ideal location to test the hypothesis of cross-hemisphere disinhibition (Pascual-Leone, Walsh and Rothwell, 2000). There is some evidence that the oculomotor network is fairly resilient to perturbations, perhaps because animals execute visually-guided saccades during the inter-trial interval; thus, it may only be in the case of more potent or widespread lesions that behavioural deficits emerge, and even then any deficits can still be surprisingly task-dependent (Peel *et al.*, 2017, 2020; Vaidya *et al.*, 2019). It is also entirely possible that effects would have been seen had cTBS been combined with a pre-existing lesion; our failure to observe cTBS-PFC effects in healthy animals may not generalize to animal models of clinical conditions. Finally, a recent meta-review (Kirkovski *et al.*, 2023) on cTBS protocols emphasized that cTBS-PFC effects are more variable than cTBS-M1, perhaps due to inherent variability in both task-related activity and in PFC activity more generally (Cowley *et al.*, 2020; Khanna, Scott and Smith, 2020). Such variability in PFC activity may thus be a doubled-edge sword that influences both the ability of cTBS to influence outcome measures, and the ability to differentiate such outcome measures from noise.

Finally, and inherent to many studies with NHP, it is possible that the two NHPs in this study were simply non-responders. While non-responder rates in NHPs have not been documented to our knowledge, non-responder rates in humans to TBS range between 30% to 50% (López-Alonso *et al.*, 2014; Huang *et al.*, 2017; Boucher *et al.*, 2021; Ozdemir *et al.*, 2021). If these rates generalize to NHPs, then the chances that both our NHPs are non-responders is ~10% to 25%. However, evidence in humans from M1 suggests that a given individual may respond to TBS on some days but not others (Perellón-Alfonso *et al.*, 2018; Boucher *et al.*, 2021). Therefore, the limitations of our

small sample size is counterbalanced by repeated sampling of the same subject across many days, mitigating concerns about non-responders. Finally, analyses motivated by the possibility of the effectiveness of cTBS on some days but not others failed to reveal anything unique for cTBS-PFC (Fig 4, Table 1).

Conclusions

Our findings offer no support for the widely held assumptions that cTBS, at least of the PFC, will inhibit neural activity within the stimulated area, and consequently disinhibit neural activity in the mirroring, contralateral target. Despite using a within-subject design across numerous sessions, any behavioural or neural changes after cTBS of the PFC were indistinguishable from those following cTBS to M1 or a SHAM form of cTBS. Our results challenge the simple 'rebalancing' logic often applied for cTBS, at least to the healthy brain, and are in line with recent work showing limited reliability and reproducibility after cTBS of M1. More work is needed to better understand the effects of repetitive modes of TMS, including cTBS, on brain and behaviour in human and animal models.

Supplementary Materials

Supplementary Materials S1. Single-pulse TMS over the hand area of right M1 in awake monkey Bu reliably evoked highly localized contra-lateral thumb twitches. The example shown in this video confirms the suitability of the neuronavigation approach prior to cTBS (see methods). The single pulses in this video (audible as distinct clicks) were delivered at 30% of stimulator output, matching the intensity used for cTBS over the same site (M1) or PFC in subsequent recording sessions. Note the specificity of the motor response to the thumb, irrespective of hand and arm posture.

References

Adam, R. *et al.* (2020) ‘Functional reorganization during the recovery of contralesional target selection deficits after prefrontal cortex lesions in macaque monkeys’, *NeuroImage*, 207, p. 116339. Available at: https://doi.org/10.1016/j.neuroimage.2019.116339.

Adam, R., Johnston, K. and Everling, S. (2019) ‘Recovery of contralesional saccade choice and reaction time deficits after a unilateral endothelin-1-induced lesion in the macaque caudal prefrontal cortex’, *Journal of Neurophysiology*, 122(2), pp. 672–690. Available at: https://doi.org/10.1152/jn.00078.2019.

Alekseichuk, I. *et al.* (2019) ‘Comparative modeling of transcranial magnetic and electric stimulation in mouse, monkey, and human’, *NeuroImage*, 194, pp. 136–148. Available at: https://doi.org/10.1016/j.neuroimage.2019.03.044.

Amaya, F. *et al.* (2010) ‘Transcranial magnetic stimulation and PAS-induced cortical neuroplasticity in the awake rhesus monkey’, *Clinical Neurophysiology*, 121(12), pp. 2143–2151. Available at: https://doi.org/10.1016/j.clinph.2010.03.058.

Backen, T., Treue, S. and Martinez-Trujillo, J.C. (2018) ‘Encoding of Spatial Attention by Primate Prefrontal Cortex Neuronal Ensembles’, *eneuro*, 5(1), p. ENEURO.0372-16.2017. Available at: https://doi.org/10.1523/ENEURO.0372-16.2017.

Balan, P.F. *et al.* (2017) ‘Selective TMS-induced modulation of functional connectivity correlates with changes in behavior’, *NeuroImage*, 149, pp. 361–378. Available at: https://doi.org/10.1016/j.neuroimage.2017.01.076.

Bergmann, T.O. and Hartwigsen, G. (2020) ‘Inferring Causality from Noninvasive Brain Stimulation in Cognitive Neuroscience’, *Journal of Cognitive Neuroscience*, pp. 1–29. Available at: https://doi.org/10.1162/jocn_a_01591.

Beynel, L. *et al.* (2014) ‘What saccadic eye movements tell us about TMS-induced neuromodulation of the DLPFC and mood changes: a pilot study in bipolar disorders’, *Frontiers in Integrative Neuroscience*, 8. Available at: https://doi.org/10.3389/fnint.2014.00065.

Beynel, L. *et al.* (2019) ‘Effects of online repetitive transcranial magnetic stimulation (rTMS) on cognitive processing: A meta-analysis and recommendations for future studies’, *Neuroscience & Biobehavioral Reviews*, 107, pp. 47–58. Available at: https://doi.org/10.1016/j.neubiorev.2019.08.018.

Blumberger, D.M. *et al.* (2018) ‘Effectiveness of theta burst versus high-frequency repetitive transcranial magnetic stimulation in patients with depression (THREE-D): a randomised non-inferiority trial’, *The Lancet*, 391(10131), pp. 1683–1692. Available at: https://doi.org/10.1016/S0140-6736(18)30295-2.

Boucher, P.O. *et al.* (2021) ‘Sham-derived effects and the minimal reliability of theta burst stimulation’, *Scientific Reports*, 11(1), p. 21170. Available at: https://doi.org/10.1038/s41598-021-98751-w.

Bruce, C.J. *et al.* (1985) ‘Primate frontal eye fields. II. Physiological and anatomical correlates of electrically evoked eye movements’, *Journal of Neurophysiology*, 54(3), pp. 714–734. Available at: https://doi.org/10.1152/jn.1985.54.3.714.

Brunoni, A.R. *et al.* (2017) ‘Repetitive Transcranial Magnetic Stimulation for the Acute Treatment of Major Depressive Episodes: A Systematic Review With Network Meta-analysis’, *JAMA Psychiatry*, 74(2), p. 143. Available at: https://doi.org/10.1001/jamapsychiatry.2016.3644.

Bullock, K.R. *et al.* (2017) ‘Visual and presaccadic activity in area 8Ar of the macaque monkey lateral prefrontal cortex’, *Journal of Neurophysiology*, 118(1), pp. 15–28. Available at: https://doi.org/10.1152/jn.00278.2016.

Cameron, I.G.M., Riddle, J.M. and D’Esposito, M. (2015) ‘Dissociable Roles of Dorsolateral Prefrontal Cortex and Frontal Eye Fields During Saccadic Eye Movements’, *Frontiers in Human Neuroscience*, 9. Available at: https://doi.org/10.3389/fnhum.2015.00613.

Cohen, J.Y. *et al.* (2010) ‘Cooperation and Competition among Frontal Eye Field Neurons during Visual Target Selection’, *The Journal of Neuroscience*, 30(9), pp. 3227–3238. Available at: https://doi.org/10.1523/JNEUROSCI.4600-09.2010.

Cowley, B.R. *et al.* (2020) ‘Slow Drift of Neural Activity as a Signature of Impulsivity in Macaque Visual and Prefrontal Cortex’, *Neuron*, 108(3), pp. 551-567.e8. Available at: https://doi.org/10.1016/j.neuron.2020.07.021.

Dash, S. *et al.* (2018) ‘Frontal Eye Field Inactivation Reduces Saccade Preparation in the Superior Colliculus but Does Not Alter How Preparatory Activity Relates to Saccades of a Given Latency’, *eneuro*, 5(2), p. ENEURO.0024-18.2018. Available at: https://doi.org/10.1523/ENEURO.0024-18.2018.

De Lima-Pardini, A.C. *et al.* (2023) ‘Transcranial magnetic stimulation in non-human primates: A systematic review’, *Neuroscience & Biobehavioral Reviews*, 152, p. 105273. Available at: https://doi.org/10.1016/j.neubiorev.2023.105273.

Di Lazzaro, V. *et al.* (2005) ‘Theta-burst repetitive transcranial magnetic stimulation suppresses specific excitatory circuits in the human motor cortex: Theta-burst repetitive transcranial magnetic stimulation’, *The Journal of Physiology*, 565(3), pp. 945–950. Available at: https://doi.org/10.1113/jphysiol.2005.087288.

Di Lazzaro, V. *et al.* (2010) ‘The effects of motor cortex rTMS on corticospinal descending activity’, *Clinical Neurophysiology*, 121(4), pp. 464–473. Available at: https://doi.org/10.1016/j.clinph.2009.11.007.

Dias, E.C., Kiesau, M. and Segraves, M.A. (1995) ‘Acute activation and inactivation of macaque frontal eye field with GABA-related drugs’, *Journal of Neurophysiology*, 74(6), pp. 2744–2748. Available at: https://doi.org/10.1152/jn.1995.74.6.2744.

Dias, E.C. and Segraves, M.A. (1999) ‘Muscimol-Induced Inactivation of Monkey Frontal Eye Field: Effects on Visually and Memory-Guided Saccades’, *Journal of Neurophysiology*, 81(5), pp. 2191–2214. Available at: https://doi.org/10.1152/jn.1999.81.5.2191.

Edwards, J.D. *et al.* (2024) ‘A translational roadmap for transcranial magnetic and direct current

stimulation in stroke rehabilitation: Consensus-based core recommendations from the third stroke recovery and rehabilitation roundtable', *International Journal of Stroke*, 19(2), pp. 145–157. Available at: https://doi.org/10.1177/17474930231203982.

Everling, S. and DeSouza, J.F.X. (2005) 'Rule-dependent Activity for Prosaccades and Antisaccades in the Primate Prefrontal Cortex', *Journal of Cognitive Neuroscience*, 17(9), pp. 1483–1496. Available at: https://doi.org/10.1162/0898929054985455.

Everling, S., Dorris, M.C. and Munoz, D.P. (1998) 'Reflex Suppression in the Anti-Saccade Task Is Dependent on Prestimulus Neural Processes', *Journal of Neurophysiology*, 80(3), pp. 1584–1589. Available at: https://doi.org/10.1152/jn.1998.80.3.1584.

Fitzgerald, P., Fountain, S. and Daskalakis, Z. (2006) 'A comprehensive review of the effects of rTMS on motor cortical excitability and inhibition', *Clinical Neurophysiology*, 117(12), pp. 2584–2596. Available at: https://doi.org/10.1016/j.clinph.2006.06.712.

Franca, M. *et al.* (2006) 'Effects of theta burst stimulation protocols on phosphene threshold', *Clinical Neurophysiology*, 117(8), pp. 1808–1813. Available at: https://doi.org/10.1016/j.clinph.2006.03.019.

George, M.S. *et al.* (2010) 'Daily Left Prefrontal Transcranial Magnetic Stimulation Therapy for Major Depressive Disorder: A Sham-Controlled Randomized Trial', *Archives of General Psychiatry*, 67(5), p. 507. Available at: https://doi.org/10.1001/archgenpsychiatry.2010.46.

Gerits, A. *et al.* (2011) 'Transcranial magnetic stimulation of macaque frontal eye fields decreases saccadic reaction time', *Experimental Brain Research*, 212(1), pp. 143–152. Available at: https://doi.org/10.1007/s00221-011-2710-3.

Gu, C. and Corneil, B.D. (2014) 'Transcranial Magnetic Stimulation of the Prefrontal Cortex in Awake Nonhuman Primates Evokes a Polysynaptic Neck Muscle Response That Reflects Oculomotor Activity at the Time of Stimulation', *Journal of Neuroscience*, 34(44), pp. 14803–14815. Available at: https://doi.org/10.1523/JNEUROSCI.2907-14.2014.

Hamada, M. *et al.* (2013) 'The Role of Interneuron Networks in Driving Human Motor Cortical Plasticity', *Cerebral Cortex*, 23(7), pp. 1593–1605. Available at: https://doi.org/10.1093/cercor/bhs147.

Hanlon, C.A. *et al.* (2015) 'What goes up, can come down: Novel brain stimulation paradigms may attenuate craving and craving-related neural circuitry in substance dependent individuals', *Brain Research*, 1628, pp. 199–209. Available at: https://doi.org/10.1016/j.brainres.2015.02.053.

Héroux, M.E., Taylor, J.L. and Gandevia, S.C. (2015) 'The Use and Abuse of Transcranial Magnetic Stimulation to Modulate Corticospinal Excitability in Humans', *PLOS ONE*. Edited by F. Tremblay, 10(12), p. e0144151. Available at: https://doi.org/10.1371/journal.pone.0144151.

Hordacre, B. *et al.* (2017) 'Variability in neural excitability and plasticity induction in the human cortex: A brain stimulation study', *Brain Stimulation*, 10(3), pp. 588–595. Available at: https://doi.org/10.1016/j.brs.2016.12.001.

Huang, Y.-Z. *et al.* (2005) 'Theta Burst Stimulation of the Human Motor Cortex', *Neuron*, 45(2), pp. 201–206. Available at: https://doi.org/10.1016/j.neuron.2004.12.033.

Huang, Y.-Z. *et al.* (2017) ‘Plasticity induced by non-invasive transcranial brain stimulation: A position paper’, *Clinical Neurophysiology*, 128(11), pp. 2318–2329. Available at: https://doi.org/10.1016/j.clinph.2017.09.007.

Johnston, K., Lomber, S.G. and Everling, S. (no date) ‘Unilateral deactivation of macaque dorsolateral prefrontal cortex induces biases in stimulus selection’, *J Neurophysiol*, p. 9.

Kang, J.I. *et al.* (2016) ‘Frontostriatal Connectivity Changes in Major Depressive Disorder After Repetitive Transcranial Magnetic Stimulation: A Randomized Sham-Controlled Study’, *The Journal of Clinical Psychiatry*, 77(09), pp. e1137–e1143. Available at: https://doi.org/10.4088/JCP.15m10110.

Khanna, S.B., Scott, J.A. and Smith, M.A. (2020) ‘Dynamic shifts of visual and saccadic signals in prefrontal cortical regions 8Ar and FEF’, *Journal of Neurophysiology*, 124(6), pp. 1774–1791. Available at: https://doi.org/10.1152/jn.00669.2019.

Kirkovski, M. *et al.* (2023) ‘A systematic review of the neurobiological effects of theta-burst stimulation (TBS) as measured using functional magnetic resonance imaging (fMRI)’, *Brain Structure and Function*, 228(3–4), pp. 717–749. Available at: https://doi.org/10.1007/s00429-023-02634-x.

Klink, P.C. *et al.* (2021) ‘Combining brain perturbation and neuroimaging in non-human primates’, *NeuroImage*, 235, p. 118017. Available at: https://doi.org/10.1016/j.neuroimage.2021.118017.

Kubanek, J. *et al.* (2020) ‘Remote, brain region–specific control of choice behavior with ultrasonic waves’, *Science Advances*, 6(21), p. eaaz4193. Available at: https://doi.org/10.1126/sciadv.aaz4193.

Kunimatsu, J. *et al.* (2015) ‘Application of radiosurgical techniques to produce a primate model of brain lesions’, *Frontiers in Systems Neuroscience*, 9. Available at: https://doi.org/10.3389/fnsys.2015.00067.

Lefaucheur, J.-P. *et al.* (2014) ‘Evidence-based guidelines on the therapeutic use of repetitive transcranial magnetic stimulation (rTMS)’, *Clinical Neurophysiology*, 125(11), pp. 2150–2206. Available at: https://doi.org/10.1016/j.clinph.2014.05.021.

Lefaucheur, J.-P. *et al.* (2020) ‘Evidence-based guidelines on the therapeutic use of repetitive transcranial magnetic stimulation (rTMS): An update (2014–2018)’, *Clinical Neurophysiology*, 131(2), pp. 474–528. Available at: https://doi.org/10.1016/j.clinph.2019.11.002.

Lehmann, S.J. and Corneil, B.D. (2022) ‘Completing the puzzle: Why studies in non-human primates are needed to better understand the effects of non-invasive brain stimulation’, *Neuroscience & Biobehavioral Reviews*, 132, pp. 1074–1085. Available at: https://doi.org/10.1016/j.neubiorev.2021.10.040.

Li, C.-T. *et al.* (2014) ‘Efficacy of prefrontal theta-burst stimulation in refractory depression: a randomized sham-controlled study’, *Brain*, 137(7), pp. 2088–2098. Available at: https://doi.org/10.1093/brain/awu109.

Li, J. *et al.* (2016) ‘Effects of different frequencies of repetitive transcranial magnetic stimulation

on the recovery of upper limb motor dysfunction in patients with subacute cerebral infarction', *Neural Regeneration Research*, 11(10), p. 1584. Available at: https://doi.org/10.4103/1673-5374.193236.

Long, H. *et al.* (2018) 'Effects of combining high- and low-frequency repetitive transcranial magnetic stimulation on upper limb hemiparesis in the early phase of stroke', *Restorative Neurology and Neuroscience*, 36(1), pp. 21–30. Available at: https://doi.org/10.3233/RNN-170733.

López-Alonso, V. *et al.* (2014) 'Inter-individual Variability in Response to Non-invasive Brain Stimulation Paradigms', *Brain Stimulation*, 7(3), pp. 372–380. Available at: https://doi.org/10.1016/j.brs.2014.02.004.

Magnuson, J. *et al.* (2023) 'Neuromodulatory effects and reproducibility of the most widely used repetitive transcranial magnetic stimulation protocols', *PLOS ONE*. Edited by F. Tremblay, 18(6), p. e0286465. Available at: https://doi.org/10.1371/journal.pone.0286465.

Matsuta, H. *et al.* (2022) 'Continuous theta-burst stimulation to the sensorimotor cortex affects contralateral gamma-aminobutyric acid level and resting-state networks', *PLOS ONE*. Edited by B.A. Murphy, 17(8), p. e0272268. Available at: https://doi.org/10.1371/journal.pone.0272268.

Merken, L. *et al.* (2021) 'Behavioral effects of continuous theta-burst stimulation in macaque parietal cortex', *Scientific Reports*, 11(1), p. 4511. Available at: https://doi.org/10.1038/s41598-021-83904-8.

Mochizuki, H. *et al.* (2007) 'Hemoglobin concentration changes in the contralateral hemisphere during and after theta burst stimulation of the human sensorimotor cortices', *Experimental Brain Research*, 180(4), pp. 667–675. Available at: https://doi.org/10.1007/s00221-007-0884-5.

Mueller, J.K. *et al.* (2014) 'Simultaneous transcranial magnetic stimulation and single-neuron recording in alert non-human primates', *Nature Neuroscience*, 17(8), pp. 1130–1136. Available at: https://doi.org/10.1038/nn.3751.

Munoz, D.P. and Everling, S. (2004) 'Look away: the anti-saccade task and the voluntary control of eye movement', *Nature Reviews Neuroscience*, 5(3), pp. 218–228. Available at: https://doi.org/10.1038/nrn1345.

Olk, B. *et al.* (2006) 'Modulation of Antisaccades by Transcranial Magnetic Stimulation of the Human Frontal Eye Field', *Cerebral Cortex*, 16(1), pp. 76–82. Available at: https://doi.org/10.1093/cercor/bhi085.

Ozdemir, R.A. *et al.* (2021) 'Reproducibility of cortical response modulation induced by intermittent and continuous theta-burst stimulation of the human motor cortex', *Brain Stimulation*, 14(4), pp. 949–964. Available at: https://doi.org/10.1016/j.brs.2021.05.013.

Pascual-Leone, A., Walsh, V. and Rothwell, J.C. (2000) 'Transcranial magnetic stimulation in cognitive neuroscience – virtual lesion, chronometry, and functional connectivity', *Current Opinion in Neurobiology*, 10(2), pp. 232–237. Available at: https://doi.org/10.1016/S0959-4388(00)00081-7.

Peel, T.R. *et al.* (2014) 'Bilateral saccadic deficits following large and reversible inactivation of

unilateral frontal eye field', *Journal of Neurophysiology*, 111(2), pp. 415–433. Available at: https://doi.org/10.1152/jn.00398.2013.

Peel, T.R. *et al.* (2017) 'Frontal Eye Field Inactivation Diminishes Superior Colliculus Activity, But Delayed Saccadic Accumulation Governs Reaction Time Increases', *The Journal of Neuroscience*, 37(48), pp. 11715–11730. Available at: https://doi.org/10.1523/JNEUROSCI.2664-17.2017.

Peel, T.R. *et al.* (2020) 'Frontal eye field inactivation alters the readout of superior colliculus activity for saccade generation in a task-dependent manner', *Journal of Computational Neuroscience* [Preprint]. Available at: https://doi.org/10.1007/s10827-020-00760-7.

Perellón-Alfonso, R. *et al.* (2018) 'Similar effect of intermittent theta burst and sham stimulation on corticospinal excitability: A 5-day repeated sessions study', *European Journal of Neuroscience*, 48(4), pp. 1990–2000. Available at: https://doi.org/10.1111/ejn.14077.

Phillips, J.M., Johnston, K. and Everling, S. (2011) 'Effects of Anterior Cingulate Microstimulation on Pro- and Antisaccades in Nonhuman Primates', *Journal of Cognitive Neuroscience*, 23(2), pp. 481–490. Available at: https://doi.org/10.1162/jocn.2010.21482.

Pierrot-Deseilligny, C. *et al.* (2003) 'Decisional role of the dorsolateral prefrontal cortex in ocular motor behaviour', *Brain*, 126(6), pp. 1460–1473. Available at: https://doi.org/10.1093/brain/awg148.

Pierrot-Deseilligny, Ch. *et al.* (1991) 'CORTICAL CONTROL OF REFLEXIVE VISUALLY-GUIDED SACCADES', *Brain*, 114(3), pp. 1473–1485. Available at: https://doi.org/10.1093/brain/114.3.1473.

Pouget, P. *et al.* (2020) 'Neuronavigated Repetitive Transcranial Ultrasound Stimulation Induces Long-Lasting and Reversible Effects on Oculomotor Performance in Non-human Primates', *Frontiers in Physiology*, 11, p. 1042. Available at: https://doi.org/10.3389/fphys.2020.01042.

Rahnev, D. *et al.* (2013) 'Continuous theta burst transcranial magnetic stimulation reduces resting state connectivity between visual areas', *Journal of Neurophysiology*, 110(8), pp. 1811–1821. Available at: https://doi.org/10.1152/jn.00209.2013.

Ramezanpour, H. *et al.* (2024) 'Dynamics of Saccade Trajectory Modulation by Distractors: Neural Activity Patterns in the Frontal Eye Field', *The Journal of Neuroscience*, p. e0635242024. Available at: https://doi.org/10.1523/JNEUROSCI.0635-24.2024.

Rincon-Gonzalez, L. *et al.* (2016) 'Decisions in motion: vestibular contributions to saccadic target selection', *Journal of Neurophysiology*, 116(3), pp. 977–985. Available at: https://doi.org/10.1152/jn.01071.2015.

Robinson, D.A. (1972) 'Eye movements evoked by collicular stimulation in the alert monkey', *Vision Research*, 12(11), pp. 1795–1808. Available at: https://doi.org/10.1016/0042-6989(72)90070-3.

Robinson, D.A. and Fuchs, A.F. (1969) 'Eye movements evoked by stimulation of frontal eye fields.', *Journal of Neurophysiology*, 32(5), pp. 637–648. Available at: https://doi.org/10.1152/jn.1969.32.5.637.

Romero, M.C. *et al.* (2019) ‘Neural effects of transcranial magnetic stimulation at the single-cell level’, *Nature Communications*, 10(1), p. 2642. Available at: https://doi.org/10.1038/s41467-019-10638-7.

Romero, M.C. *et al.* (2022) ‘Neural effects of continuous theta-burst stimulation in macaque parietal neurons’, *eLife*, 11, p. e65536. Available at: https://doi.org/10.7554/eLife.65536.

Schiller, P.H., Sandell, J.H. and Maunsell, J.H. (1987) ‘The effect of frontal eye field and superior colliculus lesions on saccadic latencies in the rhesus monkey’, *Journal of Neurophysiology*, 57(4), pp. 1033–1049. Available at: https://doi.org/10.1152/jn.1987.57.4.1033.

Schlag, J., Dassonville, P. and Schlag-Rey, M. (1998) ‘Interaction of the Two Frontal Eye Fields Before Saccade Onset’, *Journal of Neurophysiology*, 79(1), pp. 64–72. Available at: https://doi.org/10.1152/jn.1998.79.1.64.

Schwartz, M.L. and Goldman‐Rakic, P.S. (1984) ‘Callosal and intrahemispheric connectivity of the prefrontal association cortex in rhesus monkey: Relation between intraparietal and principal sulcal cortex’, *Journal of Comparative Neurology*, 226(3), pp. 403–420. Available at: https://doi.org/10.1002/cne.902260309.

Sommer, M.A. and Tehovnik, E.J. (1997) ‘Reversible inactivation of macaque frontal eye field’, *Experimental Brain Research*, 116, pp. 229–249.

Sponheim, C. *et al.* (2021) ‘Longevity and reliability of chronic unit recordings using the Utah, intracortical multi-electrode arrays’, *Journal of Neural Engineering*, 18(6), p. 066044. Available at: https://doi.org/10.1088/1741-2552/ac3eaf.

Stagg, C.J. *et al.* (2009) ‘Polarity-Sensitive Modulation of Cortical Neurotransmitters by Transcranial Stimulation’, *The Journal of Neuroscience*, 29(16), pp. 5202–5206. Available at: https://doi.org/10.1523/JNEUROSCI.4432-08.2009.

Stefan, K. *et al.* (2008) ‘Theta-burst stimulation: Remote physiological and local behavioral after-effects’, *NeuroImage*, 40(1), pp. 265–274. Available at: https://doi.org/10.1016/j.neuroimage.2007.11.037.

Strzalkowski, N.D.J. *et al.* (2019) ‘Both 50 and 30 Hz continuous theta burst transcranial magnetic stimulation depresses the cerebellum’, *The Cerebellum*, 18(2), pp. 157–165. Available at: https://doi.org/10.1007/s12311-018-0971-0.

Suppa, A. *et al.* (2008) ‘Theta burst stimulation induces after‐effects on contralateral primary motor cortex excitability in humans’, *The Journal of Physiology*, 586(18), pp. 4489–4500. Available at: https://doi.org/10.1113/jphysiol.2008.156596.

Suppa, A. *et al.* (2016) ‘Ten Years of Theta Burst Stimulation in Humans: Established Knowledge, Unknowns and Prospects’, *Brain Stimulation*, 9(3), pp. 323–335. Available at: https://doi.org/10.1016/j.brs.2016.01.006.

Theleritis, C. *et al.* (2017) ‘Two Versus One High-Frequency Repetitive Transcranial Magnetic Stimulation Session per Day for Treatment-Resistant Depression: A Randomized Sham-Controlled Trial’, *The Journal of ECT*, 33(3), pp. 190–197. Available at: https://doi.org/10.1097/YCT.0000000000000387.

Thut, G. and Pascual-Leone, A. (2010) ‘A Review of Combined TMS-EEG Studies to Characterize Lasting Effects of Repetitive TMS and Assess Their Usefulness in Cognitive and Clinical Neuroscience’, *Brain Topography*, 22(4), pp. 219–232. Available at: https://doi.org/10.1007/s10548-009-0115-4.

Vaidya, A.R. *et al.* (2019) ‘Lesion Studies in Contemporary Neuroscience’, *Trends in Cognitive Sciences*, 23(8), pp. 653–671. Available at: https://doi.org/10.1016/j.tics.2019.05.009.

Valchev, N. *et al.* (2015) ‘cTBS delivered to the left somatosensory cortex changes its functional connectivity during rest’, *NeuroImage*, 114, pp. 386–397. Available at: https://doi.org/10.1016/j.neuroimage.2015.04.017.

Valero-Cabre, A. *et al.* (2012) ‘Frontal Non-Invasive Neurostimulation Modulates Antisaccade Preparation in Non-Human Primates’, *PLoS ONE*, 7(6), p. 11.

Valero‐Cabré, A., Pascual‐Leone, A. and Rushmore, R.J. (2008) ‘Cumulative sessions of repetitive transcranial magnetic stimulation (rTMS) build up facilitation to subsequent TMS‐mediated behavioural disruptions’, *European Journal of Neuroscience*, 27(3), pp. 765–774. Available at: https://doi.org/10.1111/j.1460-9568.2008.06045.x.

Vernet, M. *et al.* (2014) ‘Frontal eye field, where art thou? Anatomy, function, and non-invasive manipulation of frontal regions involved in eye movements and associated cognitive operations’, *Frontiers in Integrative Neuroscience*, 8(66). Available at: https://doi.org/10.3389/fnint.2014.00066.

Vink, J.J.T. *et al.* (2023) ‘Continuous Theta-Burst Stimulation of the Contralesional Primary Motor Cortex for Promotion of Upper Limb Recovery After Stroke: A Randomized Controlled Trial’, *Stroke*, 54(8), pp. 1962–1971. Available at: https://doi.org/10.1161/STROKEAHA.123.042924.

Wallis, J.D., Anderson, K.C. and Miller, E.K. (2001) ‘Single neurons in prefrontal cortex encode abstract rules’, *Nature*, 411(6840), pp. 953–956. Available at: https://doi.org/10.1038/35082081.

Wegener, S.P., Johnston, K. and Everling, S. (2008) ‘Microstimulation of monkey dorsolateral prefrontal cortex impairs antisaccade performance’, *Experimental Brain Research*, 190(4), pp. 463–473. Available at: https://doi.org/10.1007/s00221-008-1488-4.

Wischnewski, M. and Schutter, D.J.L.G. (2015) ‘Efficacy and Time Course of Theta Burst Stimulation in Healthy Humans’, *Brain Stimulation*, 8(4), pp. 685–692. Available at: https://doi.org/10.1016/j.brs.2015.03.004.

Zheng, C., Liao, W. and Xia, W. (2015) ‘Effect of combined low-frequency repetitive transcranial magnetic stimulation and virtual reality training on upper limb function in subacute stroke: a double-blind randomized controlled trail’, *Journal of Huazhong University of Science and Technology [Medical Sciences]*, 35(2), pp. 248–254. Available at: https://doi.org/10.1007/s11596-015-1419-0.

Ziemann, U. and Siebner, H.R. (2015) ‘Inter-subject and Inter-session Variability of Plasticity Induction by Non-invasive Brain Stimulation: Boon or Bane?’, *Brain Stimulation*, 8(3), pp. 662–663. Available at: https://doi.org/10.1016/j.brs.2015.01.409.